TITLE PAGE

Title. Simultaneous overexpression of human E5NT and ENTPD1 protects porcine endothelial cells against H_2O_2-induced oxidative stress and cytotoxicity *in vitro*

Author names and affiliations. Elisa Chisci[a,1], Marco De Giorgi[a,b,1], Elisa Zanfrini[a], Angela Testasecca[a], Elena Brambilla[a], Alessandro Cinti[a], Laura Farina[a], Barbara Kutryb-Zajac[b], Cristina Bugarin[c], Chiara Villa[a], Emanuela Grassilli[a], Romina Combi[a], Giuseppe Gaipa[c], Maria Grazia Cerrito[a], Ilaria Rivolta[a], Ryszard Tomasz Smolenski[b], Marialuisa Lavitrano[a], Roberto Giovannoni[a].

[a] School of Medicine and Surgery, University of Milano-Bicocca, via Cadore 48, 20900 Monza, Italy

[b] Department of Biochemistry, Medical University of Gdansk, Debinki 1, 80-211 Gdansk, Poland

[c] M. Tettamanti Research Center, Pediatric Clinic, University of Milano Bicocca, 20900 Monza, Italy

Corresponding author. Dr. Roberto Giovannoni, School of Medicine, University of Milano-Bicocca, via Cadore 48, 20900 Monza, Italy. roberto.giovannoni@unimib.it

Footnotes. [1] E.C. and M.D.G. contributed equally to this work.

Abstract

Ischemia-reperfusion injury (IRI) and oxidative stress still limit the survival of cells and organs in xenotransplantation models. Ectonucleotidases play an important role in inflammation and IRI in transplantation settings.

We tested the potential protective effects derived by the co-expression of the two main vascular ectonucleotidases, ecto-5'-nucleotidase (E5NT) and ecto nucleoside triphosphate diphosphohydrolase 1 (ENTPD1), in an *in vitro* model of H_2O_2-induced oxidative stress and cytotoxicity. We produced a dicistronic plasmid (named pCX-DI-2A) for the co-expression of human E5NT and ENTPD1 by using the F2A technology. pCX-DI-2A-transfected porcine endothelial cells simultaneously overexpressed hE5NT and hENTPD1, which were correctly processed and localized on the plasma membrane. Furthermore, such co-expression system led to the synergistic enzymatic activity of hE5NT and hENTPD1 as shown by the efficient catabolism of pro-inflammatory and pro-thrombotic extracellular adenine nucleotides along with the enhanced production of the anti-inflammatory molecule adenosine. Interestingly, we found that the hE5NT/hENTPD1 co-expression system conferred protection to cells against H_2O_2-induced oxidative stress and cytotoxicity. pCX-DI-2A-transfected cells showed reduced activation of caspase 3/7 and cytotoxicity than mock-, hE5NT- and hENTPD1-transfected cells. Furthermore, pCX-DI-2A-transfected cells showed decreased H_2O_2-induced production of ROS as compared to the other control cell lines. The cytoprotective phenotype observed in pCX-DI-2A-transfected cells was associated with higher detoxifying activity of catalase as well as increased activation of the survival signaling molecules Akt, extracellular signal-regulated kinases 1/2 (ERK1/2) and p38 mitogen-activated protein kinase (MAPK).

Our data add new insights to the protective effects of the combination of hE5NT and hENTPD1 against oxidative stress and constitute a proof of concept for testing this new genetic combination in pig-to-non-human primates xenotransplantation models.

Keywords

ecto-5'-nucleotidase

ecto nucleoside triphosphate diphosphohydrolase 1

oxidative stress

xenotransplantation

Highlights

- human E5NT and ENTPD1 genes were correctly co-expressed in porcine endothelial cells;
- hE5NT/hENTPD1 co-expression led to enhanced production of adenosine;
- hE5NT/hENTPD1 co-expression protected cells against H_2O_2-induced cytotoxicity;
- hE5NT/hENTPD1 co-expression lead to less ROS formation and more catalase activity;
- hE5NT/hENTPD1-transfected cells showed more activation of Akt, ERK1/2 and p38 kinases.

Abbreviations

E5NT or CD73, ecto-5'-nucleotidase; ENTPD1 or CD39, ecto nucleoside triphosphate diphosphohydrolase 1; ROS, reactive oxygen species; IRI, ischemia reperfusion injury; PE, phycoerythrin; PIECs, porcine iliac endothelial cells; WGA, wheat germ agglutinin; ERK1/2, extracellular signal-regulated kinases 1/2; MAPK, mitogen-activated protein kinase; CDS, coding sequence; EHNA, erythro-9-(2-hydroxy-3-nonyl) Adenine; CTRL, control: CAT, catalase; GPx, glutathione peroxidase.

Funding

This work was supported by the Ministero della Ricerca e dell'Università [FIRB- RBAP06LAHL to ML, 2011], University of Milano-Bicocca [2015-ATE-0277 to RG, 2015], European Union from

the resources of the European Regional Development Fund under the Innovative Economy Program [grant coordinated by JCET-UJ, No POIG.01.01.02-00-069/09 to RTS] and Foundation for Polish Science [TEAM/2011-8/7 to RTS].

MANUSCRIPT TEXT

1. Introduction

Purinergic signaling plays an important role in conditions of inflammation and ischemia reperfusion injury (IRI) that occur in transplantation settings [1,2]. Extracellular ATP and ADP accumulate in the sites of injury leading to pro-inflammatory and pro-thrombotic responses by signaling through P2 receptors (P2X and P2Y) on vascular and immune cells [1]. The extracellular levels of adenine nucleotides are mainly modulated by ectonucleotidases: ecto nucleoside triphosphate diphosphohydrolase 1 (ENTPD1, also known as CD39) converts ATP and ADP to AMP [3]; AMP is further dephosphorylated to adenosine by ecto-5'-nucleotidase (E5NT, also known as CD73) [3]. Extracellular adenosine exerts anti-inflammatory and anti-thrombotic effects by means of P1 receptors (A1, A2A, A2B, A3) signaling [1].

During the ischemia-reperfusion phenomenon occurring in allo- and xenotransplantation, there is a concomitant increasing production of reactive oxygen species (ROS) that cause injury via several mechanisms [4]. If not adequately scavenged, ROS can directly injure cells through membrane lipid peroxidation, enzymatic function impairment and DNA damage, eventually leading to cell death [5]. ROS can also induce up-regulation of leukocyte adhesion molecules, pro-inflammatory cytokines and chemokines in vascular endothelium and pancreatic islets [6,7]. That leads to increased leukocyte recruitment to the site of injury and subsequent immune cells activation, therefore exacerbation of inflammation and oxidative stress [4]. Leukocyte-derived free radicals contribute to injury, rejection and dysfunction of xenotransplanted heart and liver [8,9].

It has been reported that oxidative stress significantly impairs the activity of ectonucleotidases with the consequent loss of their protective functions. For instance, ROS inhibit the ectonucleotidase activity of ENTPD1 leading to loss of platelet inhibitory properties [10]. Moreover, histopathologic analyses have revealed the loss of ENTPD1 expression in the vasculature of rejected cardiac

xenografts [11]. Similarly, E5NT activity in porcine hearts or endothelial cells decreases following exposure to human blood [12]. Therefore, the loss of ectonucleotidases activity along with the consequent impaired extracellular adenine nucleotide metabolism may critically contribute to the coagulation dysregulation and exacerbated inflammation observed in xenotransplanted organs. Moreover, it has been reported that porcine endothelial cells show much lower activity of ectonucleotidases as compared to human [13,14]. Additionally, such altered extracellular nucleotide metabolism may constitute a feedback mechanism of increased ROS production because of the ATP-induced oxidative stress response in leukocytes [15]. Several evidences showed the protective effects exerted by ENTPD1 and E5NT against IRI in allo- and xenotransplantation models. It has been reported that the transgenic overexpression of ENTPD1 protects against renal, hepatic and cardiac ischemia-reperfusion and transplant vascular injury [16-19]. E5NT protects against renal, cardiac and intestinal ischemic damage via adenosine production [20-22]. Moreover, the overexpression of human E5NT in porcine endothelial cells inhibits Natural Killer-mediated cytotoxicity via adenosine production [13].

Given the reported protective effects of ENTPD1 and E5NT, we aimed to overexpress both genes by using the F2A technology [23-25] and to inquire into their combined action in a condition of ROS production, mimicking what happens in xenografted tissues during IRI. We already showed the feasibility of the F2A-mediated co-expression of ENTPD1 and E5NT in terms of their synergic enzymatic activities [26] and here, we investigated the protective role of ENTPD1/E5NT combination against oxidative stress. This study demonstrated, for the first time, the protection, mediated by activation of Akt, extracellular signal-regulated kinases 1/2 (ERK1/2) and p38 Mitogen-Activated Protein Kinase (MAPK) against H_2O_2-induced apoptosis and cytotoxicity along with an increased catalase-mediated H_2O_2 scavenging activity and decreased production of ROS in endothelial cells simultaneously overexpressing ENTPD1 and E5NT.

2. Materials and Methods

2.1. Reagents and antibodies

Restriction enzymes (New England Biolabs) were purchased from Euroclone, hydrogen peroxide (H_2O_2) and oligonucleotides (listed in Supplementary Table 1) were purchased from Sigma Aldrich. The following antibodies were used in FACS experiments: phycoerythrin (PE)-conjugated anti-human E5NT ([AD2], mouse monoclonal, BD Pharmigen, 10 µl per 5×10^5 cells in a 100µl staining volume); Alexa Fluor 647-conjugated anti-human ENTPD1 ([A1], mouse monoclonal, Life Technologies, 25µg/ml per 5×10^5 cells in a 100µl staining volume). The following primary antibodies were used in immunoblotting experiments: anti-human E5NT ([EPR6115], rabbit monoclonal, LifeSpan BioSciences, 1:500); anti-human ENTPD1 ([HPA014067], rabbit polyclonal, Sigma-Aldrich, 1:250); anti-beta-actin ([AC-15], mouse monoclonal, Sigma-Aldrich, 1:5000); anti-Akt (rabbit polyclonal, Cell Signaling Technology [#9272], 1:1000); anti-phosphoSer473-Akt (rabbit polyclonal, Cell Signaling Technology [#9271], 1:1000); anti-p44/p42 ERK1/2 ([137F5], rabbit monoclonal, Cell Signaling Technology [#4695], 1:1000); anti-phospho-p44/p42 ERK1/2 (Thr202/Tyr204, [20G11], rabbit monoclonal, Cell Signaling Technology [#4376], 1:1000); anti-p38 MAPK (rabbit polyclonal, Cell Signaling Technology [#9212], 1:1000); anti-phospho-p38 MAPK (Thr180/Tyr182, [28B10], mouse monoclonal, Cell Signaling Technology [#9216], 1:2000); anti-Vinculin ([hVIN-1], mouse monoclonal, Sigma Aldrich, 1:5000). The following primary antibodies were used in immunofluorescence experiments: anti-human E5NT ([4G4], mouse monoclonal, Novus Biologicals, 1:200); anti-human ENTPD1 ([BU61], mouse monoclonal, Santa Cruz Biotechnology, 1:200).

2.2. Dicistronic plasmid construction

The F2A sequence was obtained as previously described [27] and ligated by directional cloning into BamHI/XhoI-digested pcDNA3.1+ (Invitrogen) to produce the pcDNA3.1-F2A plasmid. hE5NT (NCBI: NM_002526.3) and hENTPD1 (NCBI: NM_001776.5) coding sequence (CDS) were sequentially cloned into the pcDNA3.1-F2A plasmid, as detailed in Supplementary Material. Briefly, with two rounds of recombinant PCR, hE5NT CDS was amplified without the stop codon and ligated upstream the F2A sequence into the pcDNA3.1-F2A plasmid. hENTPD1 CDS was PCR-amplified and ligated downstream the F2A into the pcDNA3.1-hE5NT-F2A plasmid. The dicistronic cassette hE5NT-F2A-hENTPD1 was excised by EcoRI digestion and ligated in EcoRI-linearized pCX-C1 [28] plasmid acceptor obtaining pCX-hE5NT-F2A-hENTPD1, which was named pCX-DI-2A.

pCX-hE5NT, pCX-hENTPD1 and pCX-empty plasmids, used as controls were obtained as previously described [29]. All the intermediate and final constructs were verified by restriction digestion analysis and by sequencing analyses performed on both strands using the BigDye Terminator Cycle Sequencing kit v1.1 and an automated ABI-3130 DNA sequencer (Applied Biosystems, Foster City, CA).

2.3. Cell culture, transfection, sorting and treatments

Porcine iliac artery endothelial cells (PIEC) were cultured in RPMI 1640 medium (EuroClone) supplemented with 10% FBS (Life Technologies) and 1x Penicillin-Streptomycin (EuroClone) at 37 °C and 5% CO_2. Cells were detached by using 1x trypisin/EDTA (EuroClone) when at 80-90% of confluence. PIEC cells were transfected using 10 μl of Lipofectamine 2000 (Invitrogen) with 4 μg of pCX-DI-2A, pCX-hE5NT, pCX-hENTPD1 or pCX-empty plasmid following manufacturer's

protocol. Transfected cells were selected by Neomycin (400 μg/ml, Sigma Aldrich) treatment for 2 weeks before being enriched by cell sorting.

For cell sorting experiments, transfected cells were detached by trypsin/EDTA and washed with FACS buffer (3% FBS and 0.01% NaN_3 in PBS, EuroClone). $5*10^5$ cells were then incubated for 30 min at 4°C in the dark with anti-human E5NT ([AD2], PE-conjugated) for pCX-hE5NT-transfected cells, or anti-human ENTPD1 ([A1], Alexa Fluor 647-conjugated) for pCX-hENTPD1-transfected cells or both antibodies for pCX-DI-2A-transfected cells. The excess and non-specifically bound antibodies were removed by washing with FACS buffer. Sorting was performed by using a FACSAria flow cytometer (Becton Dickinson). Post sorting FACS analysis was performed to check the purity of enriched cells. Isotype-matched control antibody staining did not reveal any signals. Mock-transfected cells were used as negative control of human E5NT and ENTPD1 staining (data not shown).

Apoptosis cell death was assessed on PIEC transfected cell lines after treatment with 100 μM H_2O_2 for 4, 6 and 8 hours or after treatment with 10 ng/ml human TNF-α (Sigma Aldrich) for 8, 16 and 24 hours. Immunoblotting analysis and cytotoxicity assay in response to hydrogen peroxide were performed on cells treated with 400 μM H_2O_2 for 2, 4 and 6 hours,. ROS generation was measured after 30, 60 and 90 minutes of 100 μM and 400 μM H_2O_2 exposure, while the GSH/GSSG ratio was measured after 30, 60 and 90 minutes of 400 μM H_2O_2 exposure. Catalase (CAT) and Glutathione Peroxidase (GPx) enzymatic assays were performed on cells treated with 400 μM H_2O_2 for 30 minutes and 2, 4 and 6 hours.

2.4. Immunoblotting

Immunoblotting analyses to detect the expression of human proteins in transfected cells were performed as previously described [27,29]. Immunoblotting analyses to evaluate the molecular response of PIEC cell lines exposed to H_2O_2 toxic insult, were performed as follows: at the end of

treatments, cells were lysed with 1X RIPA lysis buffer (50mM Tris-HCl pH 7.4, 150mM NaCl, 1% Triton X-100, 0.1 % SDS) added with 1mM DTT, 1mM EDTA and EGTA, and 1.5% Protease Inhibitor Cocktail and Phosphatase Inhibitor Cocktail, and protein extracts were quantified by Bradford assay (Sigma Aldrich), following manufacturer's instructions. Protein extracts were then loaded on NuPAGE Bis-Tris pre-casted mini gels (Life Technologies) following manufacturer instructions. Blotting onto nitrocellulose membrane (Life Technologies) was performed using iBlot System 2 (Life Technologies). After blocking, membranes were incubated with the selected primary antibody and then with the appropriate secondary antibody: anti-mouse IgG (H+L) HRP-conjugate (Alpha Diagnostic Intl. Inc.) and ECL anti-rabbit IgG HRP linked (GE Healthcare) secondary antibodies (1:5000). Super Signal West Dura Extended duration substrate (Thermo Scientific) was added to the membranes and chemiluminescent signal was digitally acquired by GBox (Syngene). Densitometric analysis of Western blot bands was performed by using "Gel analyzer" function of ImageJ software[30].

2.5. Immunofluorescence and confocal microscopy

pCX-DI-2A- and mock-transfected cells were seeded at 4×10^4 cells/well in 8-well chamber slides (LabTek Chamber slides, Thermo Fisher Scientific) for 24 hours. The next day, cells were washed with PBS and fixed with methanol-acetone 1:1 for 10 min at -20 °C. After fixation, cells were blocked with 1% BSA for 30 min. Fixed cells were co-incubated for 1 hour with either mouse anti-human E5NT or mouse anti-human ENTPD1 antibodies and plasma membrane marker Alexa Fluor 488 conjugated-wheat germ agglutinin (WGA, Thermo Fisher Scientific, 1:200). Alexa Fluor 594-conjugated anti mouse IgG (Life Technologies) was used as secondary antibody for 30 min (1:5000 in 1% BSA (w/v) PBS). Cells were then washed and counterstained with DAPI. The stained cells were mounted with mounting medium (Fluoromount; Sigma-Aldrich) and analyzed by LSM 710 confocal microscope (Zeiss). Images were acquired by ZEN 2009 software (Zeiss).

2.6. hE5NT and hENTPD1 activity assay and extracellular adenine nucleotides metabolism determination

hE5NT and hENTPD1 activity assay was performed as previously described [26,27]. Briefly, PIEC cells were pre-incubated for 15 minutes in HBSS supplemented with glucose (1 mg/ml; Sigma-Aldrich) and adenosine deaminase inhibitor, erythro-9-(2-hydroxy-3-nonyl) Adenine, EHNA (5 μM; Sigma-Aldrich). Then, cells were incubated with 50 μM AMP, or ADP, or ATP (Sigma-Aldrich) and supernatant samples were collected after 0, 5, 15, 30 minutes.

Extracellular adenine nucleotides and their metabolites were measured in supernatant samples of PIEC cells incubated with 400 μM H_2O_2 in HBSS supplemented with glucose (1 mg/mL) for 0, 5, 15, 30, 60 minutes. Samples were analyzed for nucleotide metabolite content by reversed-phase high performance liquid chromatography (RP-HPLC) as previously described [31].

2.7. Caspase 3/7 activity assay

Caspase 3/7 activity was measured by using Caspase-Glo 3/7 assay (Promega) as previously described [29]. Briefly, 10^4 PIEC cells/well were seeded in a white 96-well plate (Corning). The day after seeding, cells were treated with H_2O_2 or human TNF-α and then, lyophilized Caspase-Glo 3/7 substrate was resuspended and added to cells according to the manufacturer's protocol. Luminescent signal was measured by using a 96 multi-well plate reader (Infinite M200; Tecan).

2.8. Cytotoxicity assay

Cytotoxicity was analyzed by using SYTOX® Green Nucleic Acid Stain (Life Technologies) following the manufacturer's instructions. Briefly, 2×10^6 PIEC cells were seeded in 100mm Petri

dish (Euroclone) and exposed to H_2O_2 the next day. Then, 5×10^5 cells were collected, washed with 1X TBS (50 mM Tris-HCl, pH 7.4 and 150 mM NaCl) and incubated with 100 nM SYTOX® Green Nucleic Acid Stain for 20 minutes at 4°C in the dark. After two washes with 1X TBS, cells were resuspended in 100 µl 1X TBS and analyzed for dye incorporation by Tali® Image Cytometer (Life Technologies). Data were plotted using FlowJo Single Cell Analysis Software (http://ww.flowjo.com).

2.9. Oxidative stress measurement

For measuring ROS production, the fluorogenic probe CellROX® Orange Reagent (Life Technologies) was used. Briefly, 2×10^6 PIEC cells were seeded in 100 mm Petri dish and exposed to H_2O_2 the next day. After one wash with PBS, cells were incubated with 100 nM CellROX® Orange Reagent (Life Technologies) for 30 minutes at 37°C in the dark. After two washes with PBS, 5×10^5 cells were resuspended in 100 µl PBS and analyzed for ROS production by Tali® Image Cytometer.

Alternatively, 4×10^4 PIEC cells/well were seeded in 8-well chamber slides for fluorescent *in situ* detection. After treatment with H_2O_2, cells were incubated with 100 nM CellROX® Orange Reagent Cells for 30 minutes in the dark. Then cells were fixed with methanol-acetone 1:1 for 10 minutes at -20°C, following by one wash with PBS and nuclear staining with DAPI. Stained cells were analyzed as described above.

For measuring the GSH/GSSG ratio, the GSH/GSSG-Glo assay (Promega) was used following the manufacturer instructions. This kit allows the measurement of both oxidized and total glutathione levels in order to compute the ratios of reduced to oxidized glutathione. Briefly, 10^4 PIEC cells/well were seeded in white 96-well plate and exposed to H_2O_2 the next day. After treatment, cells were lysed with Total Gluthatione Lysis or Oxidixed Gluthatione Lysis Reagent directly in the culture plate and immediately exposed to the luciferin reaction buffer for 30

minutes at room temperature in the dark. Then, luciferin detection reagent was added to the lysates and luminescence was measured after 15 minutes of incubation by using a 96 multi-well plate reader (Infinite M200; Tecan) according to the manufacturer's protocol. Background readouts were subtracted from all measurements and standard curve was generated using Glutathione (GSH) included in the kit. Three wells per experimental group were used.

2.10. Antioxidant enzymes activity assays

CAT activity was measured by using Catalase Assay Kit (Sigma Aldrich) following the manufacturer instructions. Briefly, 2×10^6 PIEC cells were seeded in 100 mm Petri dish and exposed to H_2O_2 the next day. Cells were collected at the indicated time points and proteins were extracted as described above. 3 µl of a 2 mg/ml dilution of each protein sample were used to start the reaction in 100 µl of reaction buffer containing 50 mM H_2O_2. After 5 minutes of incubation, an aliquot of the catalase enzymatic reaction mixture was added to the Color Reagent (150 mM potassium phosphate buffer, pH 7.0, containing 0.25 mM 4-aminoantipyrine, 2 mM 3,5-dichloro-2-hydroxybenzenesulfonic acid and 0.5-0.8 U/ml peroxidase) followed by 15 minutes of incubation at room temperature in the dark. Absorbance at 520 nm was measured by using a 96 multi-well plate reader (Infinite M200; Tecan) according to the manufacturer's protocol. A standard curve was generated using a series of standard solution of H_2O_2 included in the kit.

GPx activity was measured by using Glutathione peroxidase cellular activity assay kit (Sigma Aldrich) following the manufacturer instructions with some modifications. Briefly, cell treatments and protein extraction were carried out as described above for catalase assay. 40 µg of proteins were used for measuring the GPx activity in 100 µl of reaction buffer containing 0.25 mM NADPH, 2.1 mM GSH, 0.5 U/ml glutathione reductase and 300 µM t-Bu-OOH. A standard curve was generated using Glutathione peroxidase standard (Sigma Aldrich). The kinetic decrease in absorbance at 340 nm was measured by using a 96 multi-well plate reader (Infinite M200; Tecan) according to the manufacturer's protocol.

2.11. Statistical analysis

Statistical analyses were performed with SPSS v.19 software (IBM). Data are expressed as mean ± standard error of the mean (S.E.M.). Caspase 3/7, Sytox, oxidative stress measurements and activity assays were independently performed at least 3 times. One-way ANOVA followed by Tukey's *post hoc* was used for comparing multiple experimental groups. Data were considered statistically significant when $p<0.05$.

3. Results

3.1. pCX-DI-2A-transfected cells simultaneously expressed human E5NT and ENTPD1

In order to investigate the protective effects of the simultaneous expression of human E5NT and ENTPD1 against oxidative stress, we engineered an F2A-based dicistronic plasmid encoding for both proteins and we used this plasmid for transfecting porcine iliac endothelial cells (PIECs).

The dicistronic plasmid was designed and produced with a similar strategy used for previously reported F2A-based constructs [27,29]. Briefly, the hE5NT CDS was cloned without the stop codon upstream of the F2A sequence. The hENTPD1 CDS was cloned in frame downstream of the F2A sequence and the resulting dicistronic CDS was then moved in pCX-plasmid under the control of the Citomegalovirus early enhancer/chicken beta actin promoter (pCAGGS) (Figure 1A).

PIECs were transfected with pCX-DI-2A plasmid and enriched for the expression of both hE5NT and hENTPD1 by cell sorting. Post-sorting FACS analysis showed a population of around 95% of cells double positive for hE5NT and hENTPD1 (Figure 1B). The size of the exogenously expressed hE5NT and hENTPD1 in pCX-DI-2A-transfected cells was verified by western blot analyses (Figures 1C-D). Then, we checked the subcellular localization of hE5NT and hENTPD1, which

both correctly co-localized with the plasma-membrane marker, wheat germ agglutinin (WGA) (Figures 1E-F). Single-gene expressing vectors [29] were used for transfection of PIECs as control of the effects derived by the separate expression of hE5NT and hENTPD1. After cell sorting, the purity of cells positive for either hE5NT or hENTPD1 was up to 95% (Supplementary Figure 1).

Taken together, these findings demonstrated that pCX-DI-2A plasmid mediates the simultaneous expression and the correct processing of human E5NT and ENTPD1 in porcine endothelial cells.

3.2. Synergic enzymatic activity of hE5NT and hENTPD1 in pCX-DI-2A-transfected cells

With the aim to evaluate the enzymatic activity of the simultaneously expressed hE5NT and hENTPD1, we incubated pCX-DI-2A-transfected and control cell lines with ATP, ADP or AMP and we measured the extracellular nucleotide metabolism over time by HPLC (Figure 2).

Following ATP incubation, ADP production was similar between pCX-DI-2A- and pCX-hENTPD1-transfected cells but significantly higher as compared to pCX-hE5NT- and mock-transfected cells at early time points (5 minutes, $p<0.05$, and 15 minutes, $p<0.05$; Figure 2A). pCX-hENTPD1-transfected cells showed an almost total conversion of ATP to AMP after 30 minutes of incubation (44.4±5 nmol/ml) whereas the extracellular AMP produced by pCX-DI-2A-transfected cells increased up to 15.3±3.3 nmol/ml after 15 minutes of incubation (Figure 2B). Nevertheless, pCX-DI-2A- and pCX-hENTPD1-transfected cells showed a similar rate of ATP degradation (Supplementary Figure 2A). No AMP production was revealed in pCX-hE5NT- and mock-transfected cells during the time of incubation suggesting a very low endogenous ATPase activity (Figure 2B). A significant production of adenosine (up to 28.3±2.5 nmol/ml following 30 minutes of incubation) was observed only in pCX-DI-2A-transfected cells suggesting the synergic hE5NT-mediated catabolism of the AMP produced by hENTPD1 (Figure 2C).

Following ADP incubation, pCX-hENTPD1-transfected cells showed again the highest production of AMP (44.7±1.8 nmol/ml after 30 minutes; Figure 2D), but we did not reveal the

simultaneous catabolism of AMP to adenosine in this cell line (Figure 2E). Despite a similar ADP degradation rate in pCX-DI-2A- and pCX-hENTPD1-transfected cells (Supplementary Figure 2B), pCX-DI-2A-transfected cells showed a lower accumulation of extracellular AMP as compared to pCX-hENTPD1-transfected cells (14.6±1.5 nmol/ml after 30 minutes, $p<0.05$). In pCX-DI-2A-transfected cells, AMP was indeed simultaneously converted to adenosine by hE5NT over the time of incubation (Figure 2E). Interestingly, we observed a slight production of AMP and adenosine also by pCX-hE5NT-transfected cells (Figures 2D-E).

Following AMP incubation, the production of adenosine was detected only in pCX-DI-2A- and pCX-hE5NT-transfected cells (Figure 2F). Consistently, the AMP degradation rate was similar in pCX-DI-2A- and pCX-hE5NT-transfected cells and almost absent in pCX-hENTPD1- and mock-transfected cells (Supplementary Figure 2C).

All together, these data showed that pCX-DI-2A-transfected cells not only efficiently catabolize the extracellular adenine nucleotides but also enhance the production of adenosine.

3.3. The combined expression of hE5NT and hENTPD1 proteins reduced caspase activation induced by pro-apoptotic stimuli in pCX-DI-2A-transfected cells

It has been reported that the inhibition of apoptosis can reduce the IRI [32,33]. Since during IRI, E5NT and ENTPD1 reduce free radicals [34] and exert anti-apoptotic effects [19], respectively, we investigated the potential protective role of their combination against H_2O_2-induced apoptosis by caspase 3/7 activity assay (Figure 3). pCX-DI-2A-transfected cells did not show increase of caspase 3/7 activity over time (1.08±0.001, 1.02±0.003 and 1.02±0.07 after 4, 6 and 8 hours of exposure to H_2O_2, respectively), contrarily to what observed in the other PIEC cell lines (Figure 3). Moreover, pCX-DI-2A-transfected cells showed a significant lower level of caspases activation after 6 and 8 hours of treatment (1.02±0.003 and 1.02±0.07) as compared to both pCX-hENTPD1- (2.17±0.23 and 2.17±0.19; $p<0.05$) and mock-transfected cells (2.17±0.43 and 2.3±0.35; $p<0.05$). pCX-

hE5NT-transfected cells showed only a trend of lower caspase 3/7 activity as compared to mock-transfected cells at 6 and 8 hours of H_2O_2 treatment (1.73±0.09 and 1.79±0.34; Figure 3).

To investigate whether hE5NT/hENTPD1 combination could afford protection also against other pro-inflammatory stimuli relevant in IRI, we incubated PIEC cells with 10 ng/ml human TNF-α. We observed that pCX-DI-2A-transfected cells were significantly protected against human TNF-α-induced apoptosis at 8, 16 and 24 hours of exposure as compared to mock-transfected cells (Supplementary Figure 3). Moreover, pCX-DI-2A-transfected cells showed better protection as compared to pCX-hE5NT-transfected cells at 16 and 24 hours but not as compared to pCX-hENTPD1-transfected cells (Supplementary Figures 3B-C).

These data suggest that the simultaneous expression of the two exogenous proteins better protected endothelial cells by inhibiting apoptosis induced by H_2O_2 and TNF-α.

3.4. Cytoprotection mediated by the combination hE5NT/hENTPD1 in pCX-DI-2A-transfected cells

Since during IRI, abundant ROS production and release can lead to cell toxicity and death [33], we investigated if the combined expression of hE5NT and hENTPD1 in pCX-DI-2A-transfected cells would confer protection against oxidative injury mediated by H_2O_2. To this extent, controls and transfected PIEC cells were exposed to 400μM of H_2O_2 for 2, 4 and 6 hours and the cytotoxicity was measured by Sytox incorporation assay (Figure 4).

The percentage of dead cells was notably lower in pCX-DI-2A-transfected cells than in mock-transfected cells at 2, 4 and 6 hours of treatment (9±1.73% vs. 31±1%, $p<0.05$, Figure 4D; 15.5±0.5% vs. 51±2%, $p<0.05$, Figure 4E; 23±0.58% vs. 62.5±4.5%, $p<0.05$, Figure 4F). After 2 hours of treatment, the level of cytotoxicity in pCX-hENTPD1-transfected cells (6.33±3.84%) was significantly lower than in mock-transfected cells ($p<0.05$, Figure 4D), however it underwent a strong increase after 4 and 6 hours of H_2O_2 exposure (85±1%, $p<0.05$, Figure 4E; 85.5±5.5%,

$p<0.05$, Figure 4F). pCX-hE5NT-transfected cells did not show a strong increase in percentage of dead cells after 2 and 4 hours of treatment (20.67±6.44%, Figure 4D; 30±5%, Figure 4E) but this percentage was doubled after 6 hours (42±2.83%, Figure 4F) as compared to the earliest time point. However, the cytotoxicity in pCX-hE5NT-transfected cells was significantly lower as compared to mock-transfected cells after both 4 and 6 hours of H_2O_2 exposure ($p<0.05$, Figures 4E and F). Interestingly, at the latest time point, the percentage of dead cells in pCX-DI-2A-transfected cells (23±0.58%) was significantly decreased as compared to both pCX-hE5NT- and pCX-hENTPD1-transfected cells (42±2.83% and 85.5±5.5% respectively, $p<0.05$, Figure 4F).

All together, these findings highlighted that the simultaneous expression of hE5NT and hENTPD1 had a protective effect against H_2O_2-induced cytotoxicity and that this action was more effective than the separate expression of each ectonucleotidase.

3.5. The combined activity of hE5NT and hENTPD1 resulted in catabolism of pro-inflammatory nucleotides and simultaneous production of protective adenosine in pCX-DI-2A-transfected cells during exposure to H_2O_2

To investigate the activity of the overexpressed ectonucleotidases during oxidative injury, we incubated PIEC cells with H_2O_2 and we measured the metabolism of pro-inflammatory adenine nucleotides and the production of adenosine.

Under basal conditions, we observed accumulation of extracellular ATP, ADP and AMP in mock-transfected cells (Figure 5A, C, E). pCX-hENTPD1-transfected cells showed also accumulation of AMP (Figure 5E). We detected a slight production of adenosine in pCX-hE5NT- and pCX-DI-2A-transfected cells, but not significantly different from mock- and pCX-hENTPD1-transfected cells (Figure 5G).

During H_2O_2 treatment, pCX-DI-2A-transfected cells showed efficient removal of extracellular ATP (Figure 5B) and ADP (Figure 5D), similarly to pCX-hENTPD1-transfected cells. On the

contrary, we observed accumulation of ATP in medium from mock- and pCX-hE5NT-transfected cells (Figure 5B). Mock-transfected cells also showed accumulation of ADP (Figure 5D). These data suggest very low endogenous ATPase and ADPase activity in PIEC cells that did not overexpress human ENTPD1.

Extracellular AMP accumulated in medium from mock- and pCX-hENTPD1-transfected cells whereas it was not detectable in medium from pCX-DI-2A- and pCX-hE5NT-transfected cells (Figure 5F), suggesting an efficient hE5NT-mediated AMP removal in these latter cell lines.

Interestingly, we observed significantly higher production of extracellular adenosine in medium from pCX-DI-2A-transfected cells (0.15±0.05 μmol/l after 60 minutes of incubation; Figure 5H) as compared to mock- and pCX-hENTPD1-transfected cells. pCX-hE5NT-transfected cells showed the highest production of adenosine.

Taken together, these data suggest that in conditions of H_2O_2-induced oxidative stress and cytotoxicity, pCX-DI-2A-transfected cells showed the efficient hENTPD1-mediated removal of pro-inflammatory and pro-thrombotic adenine nucleotides along with the simultaneous hE5NT-mediated production of anti-inflammatory and protective adenosine.

3.6. The combined expression of hE5NT and hENTPD1 reduced H_2O_2-induced ROS formation in pCX-DI-2A-transfected cells

Having demonstrated that pCX-DI-2A-transfected showed an increased conversion of pro-inflammatory nucleotides to adenosine even in presence of H_2O_2 and, at the same time, were protected against H_2O_2-mediated cell toxicity, we further investigated whether this effect was due to a lower ROS production within the cells. Cells were exposed to 100 μM H_2O_2 and cellular ROS were detected *in situ* by CellROX® Orange Reagent (Supplementary Figure 4). Only mock-transfected cells showed a well-defined staining already after 30 minutes of treatment (Supplementary figure 4A), whereas a marked signal was observed in both single gene-transfected

cell lines only after 60 and 90 minutes of incubation (Supplementary figures 4B and C). pCX-DI-2A-transfected showed less stained cells with slight intensity as compared to all the other cell lines at every time points (Supplementary Figures 4).

Then, we assessed ROS generation following treatment with a cytotoxic concentration of H_2O_2 (400 μM). pCX-DI-2A-transfected cells were still protected from ROS formation as shown by the fewer and less stained cells as compared to all the other cell lines after 90 minutes of incubation (Figure 6). As expected, the generation of ROS was lower in all the PIEC cell lines after 30 and 60 minutes exposure to H_2O_2 (Supplementary Figures 5A and B) as compared to 90 minutes of treatment (Figure 6) and an increase in signal intensity was observed over time, prompting a progressive formation of ROS within cells.

In order to accurately quantify the production of ROS into the cells, PIEC cell lines were treated for 30, 60 or 90 minutes with 400 μM of H_2O_2 and the CellROX® Orange Reagent-positive cells were measured by Tali® Image Cytometer. As shown in Figure 7, ROS formation was significantly lower in pCX-DI-2A-transfected cells than in mock-transfected cells at 30, 60 and 90 minutes of treatment (5.63±2.22% vs. 99.8±0.17%, $p<0.05$, Figure 7A; 31.2±9.48% vs. 98.9±0.95%, $p<0.05$, Figure 7B; 31.4±9.55% vs. 99.7±0.27%, $p<0.05$, Figure 7C). Similarly, after 30 minutes of H_2O_2 exposure, pCX-hE5NT- and pCX-hENTPD1-transfected cells showed a significantly reduced ROS formation (3.47±2.03% and 0.33±0.24%, respectively) as compared to mock-transfected cells ($p<0.05$, Figure 7A). However, the levels of cellular ROS underwent a remarkable increase after 60 and 90 minutes of treatment in both the pCX-hE5NT- (73.4±18.16%, Figure 7B; 81.4±14.35%, Figure 7C) and pCX-hENTPD1-transfected cell lines (58.1±17.07%, Figure 7B; 77.45±1.25%, Figure 7C) as compared to the earliest time point ($p<0.05$ for each cell line). Interestingly, despite the high ROS formation in pCX-hENTPD1-transfected cells at 90 minutes of treatment, it was still significantly lower than the level of ROS in mock-transfected cells (Figure 7C, $p<0.05$).

Noteworthy, after 60 and 90 minutes of H_2O_2 treatment, pCX-DI-2A-transfected cells produced a reduced level of ROS as compared to all the other cell lines ($p<0.05$, Figures 7B and C).

Additionally, we measured the GSH/GSSG ratio in PIEC cells as an indicator of oxidative stress following exposure to H_2O_2 (Supplementary figure 6). However, we did not observe differences in the GSH/GSSG ratio modulation between the cell lines at every time points of treatment. (Supplementary figure 6).

Taken together, these data showed the involvement of hE5NT and hENTPD1 in the process of H_2O_2-induced cellular ROS generation, and suggest that their combined action protects pCX-DI-2A-transfected cells against the toxic formation of ROS.

3.7. pCX-DI-2A-transfected cells showed enhanced H_2O_2 scavenging activity mediated by catalase

In order to unravel the hE5NT/hENTPD1-mediated activation of downstream pathways accounting for the protection against H_2O_2–induced toxicity and ROS generation, we first focused our attention on H_2O_2 metabolism. Cellular antioxidant systems, such as CAT and GPx, protect cells from H_2O_2-induced oxidative stress. Therefore, we evaluated the enzymatic activity of CAT and GPx in PIEC cell lines treated with 400 µM H_2O_2 for 30, 120, 240 and 360 minutes (Figure 8 and Supplementary figure 7).

As shown in Figure 8, CAT activity was two fold higher in pCX-DI-2A-transfected cells as compared to mock-transfected cells in basal condition (102±4.3 U/ml/µg vs.51.6±3.4 U/ml/µg, $p<0.05$).

Under H_2O_2 exposure, pCX-DI-2A-transfected cells showed a significantly higher CAT activity than mock-transfected cells at every time points (89.1±3.3 U/ml/µg vs. 45.8±8.8 U/ml/µg at 30 minutes; 126.8 ±1.5 U/ml/µg vs. 51.4±17.8 U/ml/µg at 120 minutes; 132.5±9.2 U/ml/µg vs. 29.6±2.5 U/ml/µg at 240 minutes; 135.5±18.6 U/ml/µg vs. 2.5±0.3 U/ml/µg at 360 minutes; $p<0.05$; Figure 8).

Interestingly, pCX-DI-2A-transfected cells showed also a significantly higher CAT activity than pCX-hE5NT-transfected cells (69.1±17.6 U/ml/µg for untreated cells; 61.3±2.4 U/ml/µg at 30

minutes; 69.1±4.1 U/ml/µg at 120 minutes; 84.1±8.2 U/ml/µg at 240 minutes; 60.5±5.3 U/ml/µg at 360 minutes; $p<0.05$; Figure 8) and pCX-hENTPD1-transfected cells (49.4±12.6 U/ml/µg for untreated cells; 52.0±1.6 U/ml/µg at 30 minutes; 46.5±2.6 U/ml/µg at 120 minutes; 43.1±4.3 U/ml/µg at 240 minutes; 3.6±1.0 U/ml/µg at 360 minutes; $p<0.05$; Figure 8). Moreover, pCX-hE5NT-transfected cells showed a greater CAT activity than both mock- and pCX-hENTPD1-transfected cells after 240 and 360 minutes of exposure to H_2O_2 (84.1±8.2 U/ml/µg vs 29.6±2.5 U/ml/µg and 60.5±5.3 U/ml/µg vs. 2.5±0.3 U/ml/µg, respectively, $p<0.05$; Figure 8). No relevant differences were observed between mock- and pCX-hENTPD1-transfected cells at every condition tested (Figure 8).

Then, we measured the enzymatic activity of GPx in PIEC cells treated with H_2O_2. However, we did not detect relevant activity at every condition tested and no differences between all the cell lines (Supplementary figure 7).

Overall, these findings indicated that the protective effect mediated by the combined overexpression of hE5NT and hENTPD1 against H_2O_2-induced oxidative stress may be due to a high catalase activity, which remained constant over time.

3.8. Overexpression of hE5NT and hENTPD1 modulated MAPKs molecular pathway in cells exposed to H_2O_2-induced oxidative injury

Given the role of MAPKs in the regulation of cell proliferation, survival and metabolism in response to H_2O_2 injury, we evaluated the modulation of MAPKs in cells overexpressing hE5NT and hENTPD1. To this extent, the expression of total and phosphorylated Akt, ERK1/2, p38 proteins was assessed by western blot analyses on PIEC cell lines treated with 400 µM H_2O_2 for 2, 4 and 6 hours (Figure 9).

Phosphorylated Akt (p-Akt) showed a remarkable induction in pCX-DI-2A-transfected cells as compared to mock-transfected cells (CTRL) at 2, 4 and 6 hours of treatment (1.99±0.47 vs.

0.84±0.14, $p<0.05$; 2.03±0.14 vs. 0.89±0.15, $p<0.05$; 1.65±0.40 vs. 0.43±0.03, $p<0.05$), suggesting a higher amount of activated Akt in these cells (Figures 9A and D). Furthermore, after 2 and 4 hours of H_2O_2 exposure, the p-Akt expression level was also significantly greater as compared to both pCX-hE5NT- (0.73±0.004, $p<0.05$; 0.71±0.14, $p<0.05$) and pCX-hENTPD1-transfected cells (0.80±0.07, $p<0.05$; 0.78±0.09, $p<0.05$, Figures 9A and D). No significant differences in total protein expression levels were observed in each cell line over time.

Phosphorylated ERK1/2 (p-ERK1/2) showed a significant decrease in H_2O_2 treated mock-transfected cells (CTRL) as compared to untreated cells (UT, Figure 9B $p<0.05$); p-ERK1/2 expression levels in mock-transfected cells were significantly lower than those of all other PIEC cell lines in each condition tested (Figures 9B and E, $p<0.05$). After 2, 4 and 6 hours of H_2O_2 treatment, a great induction of p-ERK1/2 was observed in pCX-hE5NT- (1.58±0.007; 2.01±0.17; 2.43±0.13) and in pCX-hENTPD1-transfected cells (1.35±0.06; 1.51±0.03; 1.86±0.24). Moreover, levels of p-ERK1/2 increased over time in both the single gene-transfected cell lines (Figures 9B and E, $p<0.05$). On the other hand, a weaker induction of ERK1/2 phosphorylation was noticed in pCX-DI-2A-transfected cells after 2 and 4 hours of H_2O_2 exposure (0.94±0.06 and 0.91±0.08, $p<0.05$) as compared to both pCX-hE5NT- and pCX-hENTPD1-transfected cells (Figures 9B and E). Total ERK1/2 protein amount was not different among the cell lines at each time point or between treated and untreated cells in each cell line (Figure 9B).

Phosphorylated form of p38 MAPK (p-p38) was almost totally abolished in H_2O_2-treated mock-transfected cells as compared to the untreated cells ($p<0.05$). Conversely, p-p38 expression levels underwent a significant increase in pCX-DI-2A-transfected cells as compared to mock-transfected cells after 2, 4 and 6 hours of H_2O_2 treatment (1.23±0.15 vs. 0.43±0.07, $p<0.05$; 1.21±0.08 vs. 0.50±0.02, $p<0.05$; 1.90±0.14 vs. 0.39±0.09, $p<0.05$; Figure 9F). Furthermore, after 6 hours of H_2O_2-exposure pCX-DI-2A-transfected cells showed a significant increase of p-p38 expression level as compared to both pCX-hE5NT- and pCX-hENTPD1-transfected cells (0.57±0.13, *$p<0.05$;* 0.80±0.08, *$p<0.05$;* respectively). Considering the change in p-p38 levels over time, pCX-DI-2A-

transfected cells showed a significant increase by comparing 6 hours and 2 hours of H_2O_2 treatment (Figure 9F, $p<0.05$). On the other hand, p38 phosphorylation did not show relevant changes in pCX-hE5NT- and pCX-hENTPD1-transfected cells over time (0.90±0.10, 1.21±0.24, 0.57±0.13 and 0.96±0.09, 0.84±0.02, 0.80±0.08 respectively, Figure 9F). Total p38 protein did not show any changes of expression level in each condition tested, as expected (Figure 9C).

Overall, these data showed that the MAPKs signaling pathway was induced in response to H_2O_2 in PIEC cells overexpressing at least one of the two human genes (ERK1/2 and p38) or both hE5NT and hENTPD1 (Akt), promoting beneficial effects that could counteract oxidative stress injury.

4. Discussion

Xenotransplantation may solve the problem of shortage of organs available for allotransplantation [35]. Despite great advances in preventing the immediate mechanisms of xenorejection [36], there are remaining immune and inflammatory barriers that still need to be overcome, such as IRI, oxidative stress and hyper-activation of coagulation [9,37,38]. Therefore, multiple additional genetic modifications are required in pig donors in order to achieve a broader protection of xenografts.

E5NT and ENTPD1 are ectonucleotidases that regulate the extracellular concentration and signaling of adenine nucleotides and adenosine [3]. Several reports showed the anti-thrombotic and anti-inflammatory effects of ENTPD1, mainly by catabolizing ATP and ADP [39,40]. On the other hand, E5NT has been demonstrated to exert anti-inflammatory and cytoprotective action through its reaction product, adenosine [39].

We report here the effects of the simultaneous expression of hE5NT and hENTPD1 (Figure 1) in porcine endothelial cells exposed to oxidative stress. We used the F2A technology to link in frame the coding sequences of human E5NT and ENTPD1 (pCX-DI-2A, Figure 1A) because of the well-documented equal expression of genes provided by the F2A sequence [23]. As expected, we

observed that pCX-DI-2A-transfected cells showed a simultaneous and comparable expression of both hE5NT and hENTPD1 proteins (Figures 1B-D) that were also correctly localized into plasma membrane (Figures 1E-F).

Furthermore, the hE5NT/hENTPD1 co-expression system resulted in the synergic enzymatic activities of hE5NT and hENTPD1. That meant the simultaneous degradation of pro-inflammatory and pro-thrombotic extracellular ATP and ADP along with the enhanced production of anti-inflammatory and immunosuppressive adenosine (Figure 2 and Supplementary Figure 2). Following incubation with ATP or ADP, only pCX-DI-2A-transfected cells showed a significant production of adenosine (Figures 2C, E). On the contrary, pCX-hENTPD1-transfected cells showed the highest accumulation of AMP, yet without a detectable production of adenosine (Figures 2B-E). The lower accumulation of AMP in pCX-DI-2A-transfected cells was associated with the observed production of adenosine (Figures 2B-E), as a result of the coordinated activity of hE5NT in catabolizing the hENTPD1-product AMP in adenosine. Following incubation with AMP, pCX-DI-2A-transfected cells showed a significant production of adenosine similarly to pCX-hE5NT-transfected cells (Figure 2F). Moreover, as we previously reported, we observed that mock-transfected cells showed very low endogenous enzymatic activity of both ectonucleotidases [13,14]. Taken together, these findings showed that pCX-DI-2A plasmid allows the efficient co-expression, correct subcellular localization and enzymatic activity of hE5NT and hENTPD1 in porcine endothelial cells.

Reactive oxygen species, such as hydroxyl radicals and superoxide anion ($O_2^{\bullet -}$) rapidly converted to hydrogen peroxide (H_2O_2) by superoxide dismutase (SOD), are generated during normal metabolic processes [41,42], and play crucial roles in cellular signaling cascades [43]. Since an imbalance between ROS production and antioxidant defense mechanisms (such as in case of IRI) induces oxidative stress and exacerbation of inflammation [33,44-46], we evaluated whether the co-expression of hE5NT and hENTPD1 could protect endothelial cells in a model of H_2O_2-induced oxidative stress and cytotoxicity. A low concentration of ROS induces apoptotic cell death if not

adequately scavenged [47]. In particular, H_2O_2-treatment results in the formation of mitochondrial permeability transition pores, a rapid decrease of the mitochondrial transmembrane potential and the release of cytochrome c, which leads in turn to the activation of effector caspase 3, therefore apoptosis [48]. The combined expression of the two ectonucleotidases, hE5NT and hENTPD1, protected pCX-DI-2A-transfected cells against H_2O_2-induced apoptosis (Figure 3). Conversely, the expression of single genes did not significantly reduce caspase 3/7 activation in pCX-hE5NT and pCX-hENTPD1-transfected cells, as compared to mock-transfected cells (Figure 3). Interestingly, pCX-hE5NT-transfected cells showed a trend of decreased activation of caspase 3/7 following 6 and 8 h of treatment with H_2O_2 as compared to mock-transfected cells (Figure 3).

On the other hand, high concentrations of H_2O_2 induce cell death mainly by necrosis [49]. We therefore evaluated the effect of the combined expression of hE5NT and hENTPD1 against the cellular cytotoxicity induced by a higher concentration of H_2O_2. Cytotoxicity results from Sytox incorporation assay pointed out a protective effect against oxidative cell injury in pCX-DI-2A- and pCX- hE5NT-transfected cells, but not in cells expressing only hENTPD1, after 4 and 6 hours of treatment (Figures 4B and E, 4C and F). Noteworthy, in pCX-DI-2A-transfected cells the beneficial effect was significantly increased as compared to both pCX-hE5NT- and pCX-hENTPD1-transfected cells (Figures 4B and E, 4C and F).

Overall, in apoptosis and cytotoxicity assays, pCX-DI-2A-transfected cells showed the highest level of protection as compared to all the other cell lines, whereas pCX-hE5NT-transfected cells showed only a partial protection. These findings suggest that hE5NT is necessary but not sufficient to confer a significant protection against the H_2O_2-induced cytotoxicity. In the attempt to investigate whether the combined enzymatic activity of hE5NT and hENPTD1 could be responsible for the observed protection in pCX-DI-2A-transfected cells, we measured the extracellular adenine nucleotides metabolism following exposure of cells to H_2O_2 (Figure 5). It is well documented that in conditions of inflammation or stress, ATP molecules are indeed actively released by cells in the extracellular milieu, where they act as paracrine danger signals [50,51]. The extracellular ATP is

mainly modulated by the combined activities of ENTPD1 and E5NT. In our experimental settings, we observed that pCX-DI-2A-transfected cells efficiently catabolized toxic and pro-inflammatory ATP and ADP and simultaneously produced protective adenosine (Figures 5B, D and H). On the contrary, pCX-hE5NT-transfected cells showed the highest production of adenosine as compared to all the other cell lines (Figure 5H), but they also showed very low ATPase activity, leading to accumulation of ATP (Figure 5B) during H_2O_2 exposure. Nonetheless, we observed that the inhibition of adenosinergic receptors by pre-treatment with caffeine did not reverse the protective responses observed in pCX-DI-2A-transfected cells against the H_2O_2-mediated damage (data not shown). Therefore, despite the observed efficient combined activity of hE5NT and hENTPD1 during H_2O_2 treatment, the adenosine receptors activation seemed not to be primarily responsible for the protection shown by pCX-DI-2A-transfected cells at least at the time points analyzed and so other protective mechanisms might be involved.

In order to elucidate these potential protective mechanisms, we then focused our attention on ROS formation. To this extent, we investigated the effects of the combination of hE5NT and hENTPD1 on the production of ROS following exposure to 100 and 400 μM H_2O_2. *In situ* analysis of PIEC cells exposed to hydrogen peroxide and stained with CellROX® Orange Reagent showed less production of ROS in pCX-DI-2A-transfected cells as compared to all the other cell lines (Figure 6 and Supplementary Figures 4-5). These data were then confirmed by the quantitative analysis of ROS production (Figure 7). On the other hand, the single expression of either hE5NT or hENTPD1 conferred significant protection only at the earliest time point (30 minutes, Figure 7A and Supplementary Figures 4 and 5), but neither of them was sufficiently protective at longer incubation times (Figure 7B-C).

Since we observed decreased ROS production in pCX-DI-2A-transfected cells following H_2O_2 treatment (Figures 6-7 and Supplementary Figures 4-5), we then evaluated the activities of H_2O_2 scavenging enzymes. The primary cellular enzymatic systems against hydrogen peroxide are the

glutathione redox cycle and catalase [52]. Glutathione peroxidase converts H_2O_2 to H_2O by oxidizing GSH to GSSG in both the cytosol and mitochondria [53]. On the other hand, catalase protects cells from the toxicity of H_2O_2 by converting it to H_2O and O_2 and it is primarily present in the peroxisome fraction [53]. We measured the GPx activity in PIEC cells treated with H_2O_2 (Supplementary Figure 7). We did not detect relevant GPx activity and any differences between all the cell lines at every time point of analysis (Supplementary Figure 7). In agreement with such findings, we also did not observe significant differences in the GSH/GSSG ratio among the cell lines following treatment with H_2O_2 (Supplementary Figure 6). Despite pCX-hENTPD1-transfected cells showed high basal GSH/GSSG ratio, we did not observe any further change following H_2O_2 exposure (Supplementary Figure 6). Further studies would be required to elucidate such behavior. Anyhow, these data suggest that the glutathione redox cycle was not primarily involved in the detoxification from H_2O_2 in our model.

On the other hand, we measured the enzymatic activity of catalase in PIEC cells exposed to H_2O_2 (Figure 8). Interestingly, we observed that pCX-DI-2A-transfected cells showed a higher catalase activity than all the other cell lines (Figure 8). We also detected that pCX-hE5NT-transfected cells showed a significantly higher catalase activity than mock- and pCX-hENTPD1-transfected cells at 240 and 360 minutes of H_2O_2 treatment (Figure 8). However, such activity was significantly lower than that one observed in pCX-DI-2A-transfected cells at each time point (Figure 8).

In accordance with such findings, the higher catalase activity correlated with the decreased formation of ROS observed in pCX-DI-2A-transfected cells (Figures 6-7 and Supplementary Figures 4-5).

It has been reported that the overexpression of human catalase protects hepatocytes from H_2O_2-induced cytotoxicity and apoptosis [52]. Similarly, the overexpression of catalase protects beta cells from the hydrogen peroxide- and streptozocin-mediated damage [54]. In agreement with such reports, pCX-DI-2A-transfected cells showed higher activity of catalase (Figure 8) along with better protection from the H_2O_2-induced apoptosis and cytotoxicity (Figures 3-4) as compared to all the

other cell lines. Furthermore, only the combined expression of hE5NT and hENTPD1 conferred enough and lasting protection to the cells against the oxidative cell damage. Moreover, these results suggest that the main intracellular ROS formation site would be the cytoplasm, where the catalase, which acts mainly at peroxisomes, is activated to mitigate the effects of hydrogen peroxide [53].

We also showed that the combination of hE5NT and hENTPD1 conferred protection against TNF-α-induced apoptosis (Supplementary Figure 3). During IRI, TNF-α is a very important mediator of the inflammatory and immune responses [55]. TNF-α is also a strong pro-apoptotic stimulus[56,57]. We previously demonstrated that the combination of hE5NT and hENTPD1 along with human heme oxygenase 1 protected fibroblasts against the TNF-α-mediated apoptosis and cytotoxicity[29]. Here, we reported that pCX-DI-2A-transfected cells showed significantly less caspase 3/7 activation as compared to mock- and pCX-hE5NT-transfected cells following TNF-α exposure (Supplementary Figure 3). Interestingly, we did not observe different caspase 3/7 activation between pCX-DI-2A- and pCX-hENTPD1-transfected cells, suggesting that the protection observed in pCX-DI-2A-transfected cells was mainly mediated by ENTPD1. Taken together, these data indicate that the combination of the two human ectonucleotidases might protect against multiple pro-apoptotic and oxidant effectors, which play a key role in the context of IRI.

We then aimed to investigate the molecular pathways of protection in pCX-DI-2A-transfected cells following exposure to H_2O_2. We examined the effect of the co-expression of hE5NT and hENTPD1 on the activation of Akt, ERK1/2 and p38 kinases (Figure 9), which are known to exert protective roles against the oxidative stress and IRI [58-60]. As shown in Figures 9A and 9D, the increase of Akt phosphorylation was significant in pCX-DI-2A-transfected cells as compared to mock-transfected cells at every time points of H_2O_2 treatment and to single gene-transfected cells after 2 and 4 hours. Martin *et al* reported a connection between H_2O_2-induced cell death and down-regulation of p-Akt by mechanisms that require the generation of ROS [61]. Consistently with this,

data from Cell Rox assay showed a great ROS production in mock-transfected cells treated with H_2O_2 and in pCX-hE5NT- and pCX-hENTPD1-transfected cells at late time points of treatment (Figures 6 and 7). The same cell lines underwent caspase 3/7 activation and cell death after 6 hours of H_2O_2 exposure (Figure 3). This effect may be due to the abundant formation of ROS, which may be involved in the downregulation of p-Akt, hence higher levels of apoptosis. On the other hand, pCX-DI-2A-transfected cells showed significantly enhanced enzymatic activity of catalase (Figure 8), which could efficiently counteract ROS generation (Figures 6, 7 and Supplementary Figures 4 and 5) as well as p-Akt down-regulation, thus resulting in the observed protection against apoptosis (Figure 3) and cytotoxicity (Figure 4).

A significant increase of phosphorylated ERK1/2 proteins was observed in pCX-E5NT-, pCX-hENTPD1- and pCX-DI-2A-transfected cells at every time point of H_2O_2 treatment as compared to mock-transfected cells (Figures 9B and 9E). However, pERK1/2 expression level was significantly lower in pCX-DI-2A-transfected cells than in pCX-E5NT- and pCX-hENTPD1-transfected cells after 2 and 4 hours of H_2O_2 exposure (Figure 9E). Recently, it has been shown that H_2O_2 exerts its effect by acting on phosphorylation-dependent activation of ERK1/2 MAP kinases, without affecting its total expression [62-64]. Moreover, although ERK1/2 activity is generally associated with cell survival, a growing body of evidence suggests that it also mediates apoptosis cell death depending on the stimulus, the cell type and the subcellular localization. For instance, Song and colleagues showed that a sustained ERK1/2 activation causes its nuclear translocation and contributes to cell death via transcriptional regulation of pro-apoptotic proteins in neural cells [63]. In this perspective, the persistence of H_2O_2 stimulus may have induced a sustained activation of ERK1/2 protein that became “toxic” over time. This effect may cause an imbalance between pro- and anti-apoptotic signals transmitted by ERK1/2, leading cells towards injurious outcomes in single gene expressing cell lines. The observed enhanced detoxifying activity of catalase in pCX-DI-2A-transfected cells (Figure 8) may prevent an excessive H_2O_2-mediated ERK1/2 phosphorylation and activation (Figure 9E), leading to resistance against apoptosis and cytotoxicity

(Figures 3-4). In fact, it has been documented that the injection of catalase mediated protection against brain IRI by abolishing ERK1/2 phosphorylation and promoting Akt phosphorylation [65].

Similarly to ERK1/2, H_2O_2 has been reported to induce phosphorylation of p38 MAPK and JNK [64], which have essential roles in the regulation of cellular responses, including cell survival and apoptosis [66]. Furthermore, activation of p38 has been reported to be involved in inducing the expression of antioxidant enzymes in human aortic endothelial cells [67]. We therefore investigated if the phosphorylation of p38 MAPK (p-p38) could have been modulated in pCX-DI-2A-transfected cells (Figures 9C and 9F). p-p38 expression levels were significantly higher in pCX-DI-2A-transfected cells at every time points of treatment as compared to mock-transfected cells. No significant increase in p-p38 was observed in single gene-transfected cells, except for pCX-hE5NT-transfected cells after 4 hours of H_2O_2 exposure (Figure 9F). Furthermore, after 6 hours, pCX-DI-2A-transfected cells showed almost a 2-fold increase in p-p38/total p38 ratio, which was significantly higher than all the other cell types (Figure 9F). It has been reported that p38 MAPK activation upregulates catalase levels during H_2O_2 treatment [68]. Consistently with this, we observed both increased p38 MAPK phosphorylation (Figure 9F) and enhanced catalase activity in pCX-DI-2A-transfected cells (Figure 8), suggesting a correlation between these two mechanisms.

5. Conclusions

The co-expression of hE5NT and hENTPD1 in pigs has been suggested to mitigate the hyperactivation of coagulation and inflammation that are observed in xenotransplantation models [69]. Here we showed for the first time that this new combination of genes conferred protection against the H_2O_2-mediated oxidative stress and cytotoxicity in porcine endothelial cells.

Furthermore, our findings further clarified the connection between the combined activity of hE5NT/hENTPD1, catalase detoxifying activity and the MAPKs signaling pathways, suggesting possible mechanisms involved in H_2O_2-mediated oxidative stress response in endothelial cells. In conclusion, our data add new insights to the protective effects of hE5NT and hENTPD1 against IRI

and constitute a proof of concept for testing this new genetic combination in pig-to-non-human primates xenotransplantation models.

Acknowledgements

The authors thank Dr. Perota at Avantea for providing the pCX-EGFP plasmid.

Figure Captions

Figure 1. pCX-DI-2A-transfected porcine endothelial cells efficiently express both hE5NT and hENTPD1. (A) Schematic map of the dicistronic pCX-DI-2A plasmid used to simultaneously express hE5NT and hENTPD1 in PIEC cells; (B) FACS analysis revealed that hE5NT (PE) and hENTPD1 (APC) were both expressed at high levels in pCX-DI-2A-transfected cells after cell sorting; (C-D) Western blotting analysis of hE5NT (C) or hENTPD1 (D) showing the expression of the human enzymes only in transfected cells; (E-F) Immunofluorescence analysis of hE5NT (red in E) or hENTPD1 (red in F) expression co-stained with plasma membrane marker WGA (green), showing the correct membrane-localization of human genes in pCX-DI-2A-transfected cells. Mock-transfected cells (ctrl) did not express human genes. DAPI (blue) was used for nuclear staining. Images in (B-F) are representative of at least 3 independent experiments.

Figure 2. Enhanced extracellular adenine nucleotide metabolism in pCX-DI-2A-transfected cells. pCX-DI-2A- (◊), pCX-hE5NT- (Δ), pCX-hENTPD1- (∇) and mock- (•) transfected cells were incubated with 50 μM ATP, or ADP, or AMP and the respective enzymatic products were measured over different time points by reverse phase HPLC. (A-C) Production of ADP (A), AMP (B) and adenosine (C) following incubation with ATP. (D-E) Production of AMP (D) and adenosine (E) following incubation with ADP. (F) Production of adenosine following incubation with AMP. Error bars represent SEM (n=3). * $p<0.05$ versus all groups; # $p<0.05$ pCX-DI-2A-transfected cells versus all groups except pCX-hENTPD1-transfected cells; § $p<0.05$ pCX-DI-2A-transfected cells versus all groups except pCX-hE5NT-transfected cells.

Figure 3. Protection against H_2O_2-induced apoptosis in pCX-DI-2A-transfected cells. pCX-DI-2A-, pCX-hE5NT-, pCX-hENTPD1- and mock-transfected (ctrl) cells were treated with 100 μM H_2O_2 for 4, 6 and 8 hours and apoptosis was measured by caspase 3/7 assay. Caspase activation in each treated cell line is expressed as a fold change value of the corresponding untreated cells. Error bars represent SEM (n≥3). * $p<0.05$ versus ctrl cells; Φ $p<0.05$ versus pCX-hENTPD1-transfected cells.

Figure 4. Protection against H_2O_2-induced cytotoxicity in pCX-DI-2A-transfected cells. pCX-DI-2A- (red), pCX-hENTPD1- (orange), pCX-hE5NT- (blue) and mock- (grey) transfected cells were treated with 400 μM H_2O_2 for 2 (A), 4 (B) and 6 (C) hours and cytotoxicity was measured by incorporation of 100 nM SYTOX Green Nucleic Acid Stain as described in Materials and Methods. Data shown in A, B and C are representative of one of three independent experiments. (D-F) Quantification of cytotoxicity after 2 (D), 4 (E) and 6 (F) hours of treatment with 400 μM H_2O_2. Cytotoxicity is expressed as the percentage of dead cells compared to the untreated sample for each cell line. Error bars in D, E and F represent SEM (n=3). * $p<0.05$ versus ctrl cells; # $p<0.05$ pCX-

DI-2A-transfected cells versus single gene-transfected cells; Φ $p<0.05$ versus pCX-hENTPD1-transfected cells. CTRL, mock-transfected cells.

Figure 5. pCX-DI-2A-transfected cells showed efficient adenine nucleotides removal and simultaneous production of adenosine during exposure to H_2O_2. pCX-DI-2A- (◊), pCX-hE5NT- (Δ), pCX-hENTPD1- (∇) and mock- (∇) transfected cells were treated with 400 μM H_2O_2 (HBSS + H_2O_2) for 60 minutes and supernatant samples were collected at 0, 5, 15, 30 and 60 minutes time points. The extracellular nucleotides content was measured by RP-HPLC. As control of the basal nucleotides and nucleosides concentration, we incubated cells with basal medium (HBSS) and we collected supernatant samples at the indicated time points. Extracellular ATP, ADP, AMP and adenosine concentration was measured in supernatant samples from PIEC cells incubated with basal medium (A, C, E, G, respectively) or medium containing H_2O_2 (B, D, F, H, respectively). Error bars represent standard deviation (n=3). * $p<0.05$ pCX-DI-2A-transfected cells versus all groups; # $p<0.05$ pCX-DI-2A- versus mock- and pCX-hE5NT-transfected cells; $ $p<0.05$ pCX-DI-2A- versus mock-transfected cells; Φ $p<0.05$ pCX-DI-2A- versus pCX-hENTPD1-transfected cells; δ $p<0.05$ pCX-DI-2A- versus mock- and pCX-hENTPD1-transfected cells.

Figure 6. pCX-DI-2A-transfected cells showed lower ROS production than control cell lines after 90 minutes exposure to H_2O_2. pCX-DI-2A-, pCX-hE5NT, pCX-hENTPD1- and mock-transfected cells were treated with 400 μM H_2O_2 for 90 minutes and ROS were detected by fluorescence staining with CellROX® Orange Reagent as described in Materials and Methods. White arrows indicate cells positive to the staining (red). Scale bar represents 100 μm. DAPI (blue) was used for nuclear staining. Images are representative of at least 3 independent experiments. CTRL, mock-transfected cells.

Figure 7. pCX-DI-2A-transfected cells were protected against H_2O_2-induced oxidative stress. pCX-DI-2A-, pCX-hE5NT-, pCX-hENTPD1- and mock-transfected cells were treated with 400 μM H_2O_2 for 30 (A), 60 (B) and 90 (C) minutes and the production of ROS levels was quantified following incubation with CellROX® Orange Reagent as described in Materials and Methods. ROS production in each treated cell line is expressed as percentage of the positive cells with respect to the corresponding untreated cells. Error bars represent SEM (n=3). * $p<0.05$ versus ctrl cells; # $p<0.05$ pCX-DI-2A-transfected cells versus single gene-transfected cells. CTRL, mock-transfected cells.

Figure 8. pCX-DI-2A-transfected cells showed higher activity of the antioxidant enzyme catalase. CAT activity was measured in untreated (UT) PIEC cells and cells treated with 400μM H_2O_2 for 30, 120, 240 and 360 minutes. Activity is expressed as enzymatic units per volume of reaction and μg of protein used for the assay. Data are presented as mean ± SEM (n=3). * $p<0.05$ versus ctrl cells; Φ $p<0.05$ versus pCX-hENTPD1-transfected cells. a $p<0.05$ pCX-DI-2A-transfected cells versus all the other cell lines; CTRL, mock-transfected cells.

Figure 9. Mitogenic signaling pathways modulation in single gene- and pCX-DI-2A-transfected cells. (A-C) Western blot analysis of lysates from pCX-DI-2A-, pCX-hE5NT-, pCX-hENTPD1 and mock-transfected cells after 2, 4, 6 hours exposure to 400 μM H_2O_2: Akt and p-Akt (A), Erk1/2 and p-Erk1/2 (B), p38 and p-p38 (C). Immunoblots are representative of 3 independent experiments. (D-F) Densitometric analysis of protein expression levels in PIEC cell lines. Data are expressed as Phospho-/Total-protein expression fold change ratio: pAkt/Akt (D), pErk1-2/Erk1-2 (E), p-p38/p38 (F). Error bars represent SEM (n=3). * $p<0.05$ versus ctrl cells; # $p<0.05$ pCX-DI-2A-transfected cells versus single gene-transfected cells. CTRL, mock-transfected cells.

6. References

[1] H.K. Eltzschig, M.V. Sitkovsky, S.C. Robson, Purinergic signaling during inflammation, N Engl J Med. 367 (2012) 2322–2333. doi:10.1056/NEJMra1205750.

[2] R. Zeiser, S.C. Robson, T. Vaikunthanathan, M. Dworak, G. Burnstock, Unlocking the Potential of Purinergic Signaling in Transplantation, Am J Transplant. (2016) n/a–n/a. doi:10.1111/ajt.13801.

[3] L.E. Baggio Savio, M. De Giorgi, S.C. Robson, Ectonucleotidases in Immunobiology, in: Encyclopedia of Immunobiology, Elsevier, 2016: pp. 424–431. doi:10.1016/B978-0-12-374279-7.02013-0.

[4] C.E. Barker, S. Ali, G. O'Boyle, J.A. Kirby, Transplantation and inflammation: implications for the modification of chemokine function, Immunology. 143 (2014) 138–145. doi:10.1111/imm.12332.

[5] W. Dröge, Free radicals in the physiological control of cell function, Physiol Rev. 82 (2002) 47–95. doi:10.1152/physrev.00018.2001.

[6] S. Lee, J. Chung, I.S. Ha, K. Yi, J.E. Lee, H.G. Kang, et al., Hydrogen peroxide increases human leukocyte adhesion to porcine aortic endothelial cells via NFkappaB-dependent up-regulation of VCAM-1, Int. Immunol. 19 (2007) 1349–1359. doi:10.1093/intimm/dxm104.

[7] S. Lee, I.S. Ha, J.H. Kim, K.S. Park, K.H. Han, S.-H. Kim, et al., Hydrogen peroxide-induced VCAM-1 expression in pancreatic islets and beta-cells through extracellular Ca2+ influx, Transplantation. 86 (2008) 1257–1266. doi:10.1097/TP.0b013e318188ab04.

[8] B.T.-T. Ngo, A. Beiras-Fernandez, C. Hammer, E. Thein, Hyperacute rejection in the xenogenic transplanted rat liver is triggered by the complement system only in the presence of leukocytes and free radical species, Xenotransplantation. 20 (2013) 177–187. doi:10.1111/xen.12035.

[9] J.-C. Charniot, D. Bonnefont-Rousselot, J.-P. Albertini, K. Zerhouni, S. Dever, I. Richard, et al., Oxidative stress implication in a new ex-vivo cardiac concordant xenotransplantation

model, Free Radic. Res. 41 (2007) 911–918. doi:10.1080/10715760701429775.

[10] S.C. Robson, E. Kaczmarek, J.B. Siegel, D. Candinas, K. Koziak, M. Millan, et al., Loss of ATP diphosphohydrolase activity with endothelial cell activation, Journal of Experimental Medicine. 185 (1997) 153–163.

[11] G.W. Byrne, A.M. Azimzadeh, M. Ezzelarab, H.D. Tazelaar, B. Ekser, R.N. Pierson, et al., Histopathologic insights into the mechanism of anti-non-Gal antibody-mediated pig cardiac xenograft rejection, Xenotransplantation. 20 (2013) 292–307. doi:10.1111/xen.12050.

[12] Z. Khalpey, A.H. Yuen, K.K. Kalsi, Z. Kochan, J. Karbowska, E.M. Slominska, et al., Loss of ecto-5'nucleotidase from porcine endothelial cells after exposure to human blood: Implications for xenotransplantation, Biochim Biophys Acta. 1741 (2005) 191–198. doi:10.1016/j.bbadis.2005.03.008.

[13] F.N. Osborne, K.K. Kalsi, C. Lawson, M. Lavitrano, M.H. Yacoub, M.L. Rose, et al., Expression of human ecto-5'-nucleotidase in pig endothelium increases adenosine production and protects from NK cell-mediated lysis, Am J Transplant. 5 (2005) 1248–1255. doi:10.1111/j.1600-6143.2005.00868.x.

[14] R.T. Smolenski, Z. Khalpey, F.N. Osborne, A. Yuen, E.M. Slominska, M. Lipiński, et al., Species differences of endothelial extracellular nucleotide metabolism and its implications for xenotransplantation, Pharmacol Rep. 58 Suppl (2006) 118–125.

[15] C.M. Cruz, A. Rinna, H.J. Forman, A.L.M. Ventura, P.M. Persechini, D.M. Ojcius, ATP activates a reactive oxygen species-dependent oxidative stress response and secretion of proinflammatory cytokines in macrophages, J Biol Chem. 282 (2007) 2871–2879. doi:10.1074/jbc.M608083200.

[16] M. Cai, Z.M. Huttinger, H. He, W. Zhang, F. Li, L.A. Goodman, et al., Transgenic over expression of ectonucleotide triphosphate diphosphohydrolase-1 protects against murine myocardial ischemic injury, J. Mol. Cell. Cardiol. 51 (2011) 927–935. doi:10.1016/j.yjmcc.2011.09.003.

[17] G. Beldi, Y. Banz, A. Kroemer, X. Sun, Y. Wu, N. Graubardt, et al., Deletion of CD39 on natural killer cells attenuates hepatic ischemia/reperfusion injury in mice, Hepatology. 51 (2010) 1702–1711. doi:10.1002/hep.23510.

[18] D.G. Wheeler, M.E. Joseph, S.D. Mahamud, W.L. Aurand, P.J. Mohler, V.J. Pompili, et al., Transgenic swine: Expression of human CD39 protects against myocardial injury, J. Mol. Cell. Cardiol. 52 (2012) 958–961. doi:10.1016/j.yjmcc.2012.01.002.

[19] S. Crikis, B. Lu, L.M. Murray-Segal, C. Selan, S.C. Robson, A.J.F. D'Apice, et al., Transgenic overexpression of CD39 protects against renal ischemia-reperfusion and transplant vascular injury, Am J Transplant. 10 (2010) 2586–2595. doi:10.1111/j.1600-6143.2010.03257.x.

[20] T. Eckle, T. Krahn, A. Grenz, D. Koehler, M. Mittelbronn, C. Ledent, et al., Cardioprotection by ecto-5 '-nucleotidase (CD73) and A(2B) adenosine receptors, Circulation. 115 (2007) 1581–1590. doi:10.1161/CIRCULATIONAHA.106.669697.

[21] A. Grenz, H. Zhang, T. Eckle, M. Mittelbronn, M. Wehrmann, C. Köhle, et al., Protective role of ecto-5'-nucleotidase (CD73) in renal ischemia, J Am Soc Nephrol. 18 (2007) 833–845. doi:10.1681/ASN.2006101141.

[22] M.L. Hart, A. Grenz, I.C. Gorzolla, J. Schittenhelm, J.H. Dalton, H.K. Eltzschig, Hypoxia-inducible factor-1α-dependent protection from intestinal ischemia/reperfusion injury involves ecto-5'-nucleotidase (CD73) and the A2B adenosine receptor, The Journal of Immunology. 186 (2011) 4367–4374. doi:10.4049/jimmunol.0903617.

[23] P. de Felipe, G.A. Luke, L.E. Hughes, D. Gani, C. Halpin, M.D. Ryan, E unum pluribus: multiple proteins from a self-processing polyprotein, Trends Biotechnol. 24 (2006) 68–75. doi:10.1016/j.tibtech.2005.12.006.

[24] A.L. Szymczak, C.J. Workman, Y. Wang, K.M. Vignali, S. Dilioglou, E.F. Vanin, et al., Correction of multi-gene deficiency in vivo using a single “self-cleaving” 2A peptide-based retroviral vector, Nat Biotechnol. 22 (2004) 589–594. doi:10.1038/nbt957.

[25] N. Fisicaro, S.L. Londrigan, J.L. Brady, E. Salvaris, M.B. Nottle, P.J. O'Connell, et al., Versatile co-expression of graft-protective proteins using 2A-linked cassettes, Xenotransplantation. 18 (2011) 121–130. doi:10.1111/j.1399-3089.2011.00631.x.

[26] M. De Giorgi, I. Pelikant-Malecka, A. Sielicka, E.M. Slominska, R. Giovannoni, A. Cinti, et al., Functional Analysis of Expression of Human Ecto-Nucleoside Triphosphate Diphosphohydrolase-1 and/or Ecto-5'-Nucleotidase in Pig Endothelial Cells, Nucleosides Nucleotides Nucleic Acids. 33 (2014) 313–318. doi:10.1080/15257770.2014.896466.

[27] M. De Giorgi, A. Cinti, I. Pelikant-Malecka, E. Chisci, M. Lavitrano, R. Giovannoni, et al., Co-expression of functional human Heme Oxygenase 1, Ecto-5′-Nucleotidase and ecto-nucleoside triphosphate diphosphohydrolase-1 by "self-cleaving" 2A peptide system, Plasmid. 79 (2015) 22–29. doi:10.1016/j.plasmid.2015.03.004.

[28] M. Okabe, M. Ikawa, K. Kominami, T. Nakanishi, Y. Nishimune, "Green mice" as a source of ubiquitous green cells, FEBS Letters. 407 (1997) 313–319. doi:10.1016/S0014-5793(97)00313-X.

[29] A. Cinti, M. De Giorgi, E. Chisci, C. Arena, G. Galimberti, L. Farina, et al., Simultaneous Overexpression of Functional Human HO-1, E5NT and ENTPD1 Protects Murine Fibroblasts against TNF-α-Induced Injury In Vitro, PLoS ONE. 10 (2015) e0141933. doi:10.1371/journal.pone.0141933.

[30] C.A. Schneider, W.S. Rasband, K.W. Eliceiri, NIH Image to ImageJ: 25 years of image analysis, Nat Methods. 9 (2012) 671–675. doi:10.1038/nmeth.2089.

[31] R.T. Smolenski, D.R. Lachno, S.J. Ledingham, M.H. Yacoub, Determination of sixteen nucleotides, nucleosides and bases using high-performance liquid chromatography and its application to the study of purine metabolism in hearts for transplantation, J. Chromatogr. 527 (1990) 414–420.

[32] M. Daemen, C. van't Veer, G. Denecker, V.H. Heemskerk, T. Wolfs, M. Clauss, et al., Inhibition of apoptosis induced by ischemia-reperfusion prevents inflammation, JCI

Insight. 104 (1999) 541–549. doi:10.1172/JCI6974.

[33] H.K. Eltzschig, T. Eckle, Ischemia and reperfusion-from mechanism to translation, Nat Med. 17 (2011) 1391–1401. doi:10.1038/nm.2507.

[34] R. Jian, Y. Sun, Y. Wang, J. Yu, L. Zhong, P. Zhou, CD73 protects kidney from ischemia-reperfusion injury through reduction of free radicals, Apmis. 120 (2012) 130–138. doi:10.1111/j.1600-0463.2011.02827.x.

[35] B. Ekser, D.K.C. Cooper, A.J. Tector, The need for xenotransplantation as a source of organs and cells for clinical transplantation, Int J Surg. 23 (2015) 199–204. doi:10.1016/j.ijsu.2015.06.066.

[36] B. Ekser, A.J. Tector, D.K.C. Cooper, Progress toward clinical xenotransplantation, Int J Surg. 23 (2015) 197–198. doi:10.1016/j.ijsu.2015.08.036.

[37] D.K.C. Cooper, B. Ekser, A.J. Tector, Immunobiological barriers to xenotransplantation, Int J Surg. 23 (2015) 211–216. doi:10.1016/j.ijsu.2015.06.068.

[38] M. Ezzelarab, B. Ekser, A. Azimzadeh, C.C. Lin, Y. Zhao, R. Rodriguez, et al., Systemic inflammation in xenograft recipients precedes activation of coagulation, Xenotransplantation. 22 (2015) 32–47. doi:10.1111/xen.12133.

[39] L. Antonioli, P. Pacher, E.S. Vizi, G. Haskó, CD39 and CD73 in immunity and inflammation, Trends in Molecular Medicine. 19 (2013) 355–367. doi:10.1016/j.molmed.2013.03.005.

[40] B. Atkinson, K. Dwyer, K. Enjyoji, S.C. Robson, Ecto-nucleotidases of the CD39/NTPDase family modulate platelet activation and thrombus formation: Potential as therapeutic targets, Blood Cells Mol Dis. 36 (2006) 217–222. doi:10.1016/j.bcmd.2005.12.025.

[41] V.J. Thannickal, B.L. Fanburg, Reactive oxygen species in cell signaling, Am J Physiol Lung Cell Mol Physiol. 279 (2000) L1005–28.

[42] B. Halliwell, Reactive oxygen species in living systems: source, biochemistry, and role in

human disease, Am. J. Med. 91 (1991) 14S–22S.

[43] M. Reth, Hydrogen peroxide as second messenger in lymphocyte activation, Nat. Immunol. 3 (2002) 1129–1134. doi:10.1038/ni1202-1129.

[44] M. Valko, D. Leibfritz, J. Moncol, M.T.D. Cronin, M. Mazur, J. Telser, Free radicals and antioxidants in normal physiological functions and human disease, Int J Biochem Cell Biol. 39 (2007) 44–84. doi:10.1016/j.biocel.2006.07.001.

[45] M. Salvadori, G. Rosso, E. Bertoni, Update on ischemia-reperfusion injury in kidney transplantation: Pathogenesis and treatment, World J Transplant. 5 (2015) 52–67. doi:10.5500/wjt.v5.i2.52.

[46] W. Zhang, M. Wang, H.Y. Xie, L. Zhou, X.Q. Meng, J. Shi, et al., Role of reactive oxygen species in mediating hepatic ischemia-reperfusion injury and its therapeutic applications in liver transplantation, Transplant Proc. 39 (2007) 1332–1337. doi:10.1016/j.transproceed.2006.11.021.

[47] H.-U. Simon, A. Haj-Yehia, F. Levi-Schaffer, Role of reactive oxygen species (ROS) in apoptosis induction, Apoptosis. 5 (2000) 415–418.

[48] M. Higuchi, T. Honda, R.J. Proske, E.T. Yeh, Regulation of reactive oxygen species-induced apoptosis and necrosis by caspase 3-like proteases, Oncogene. 17 (1998) 2753–2760. doi:10.1038/sj.onc.1202211.

[49] Y. Saito, K. Nishio, Y. Ogawa, J. Kimata, T. Kinumi, Y. Yoshida, et al., Turning point in apoptosis/necrosis induced by hydrogen peroxide, Free Radic. Res. 40 (2009) 619–630. doi:10.1080/10715760600632552.

[50] A. Gombault, L. Baron, I. Couillin, ATP release and purinergic signaling in NLRP3 inflammasome activation, Front Immunol. 3 (2012) 414. doi:10.3389/fimmu.2012.00414.

[51] S. Carta, F. Penco, R. Lavieri, A. Martini, C.A. Dinarello, M. Gattorno, et al., Cell stress increases ATP release in NLRP3 inflammasome-mediated autoinflammatory diseases, resulting in cytokine imbalance, Proceedings of the National Academy of Sciences. 112

(2015) 2835–2840. doi:10.1073/pnas.1424741112.

[52] J. Bai, A.M. Rodriguez, J.A. Melendez, A.I. Cederbaum, Overexpression of catalase in cytosolic or mitochondrial compartment protects HepG2 cells against oxidative injury, J Biol Chem. 274 (1999) 26217–26224.

[53] C.J. Weydert, J.J. Cullen, Measurement of superoxide dismutase, catalase and glutathione peroxidase in cultured cells and tissue, Nature Protocols. 5 (2010) 51–66. doi:10.1038/nprot.2009.197.

[54] B. Xu, J.T. Moritz, P.N. Epstein, Overexpression of catalase provides partial protection to transgenic mouse beta cells, Free Radic. Biol. Med. 27 (1999) 830–837.

[55] H.K. Saini, Y.-J. Xu, M. Zhang, P.P. Liu, L.A. Kirshenbaum, N.S. Dhalla, Role of tumour necrosis factor-alpha and other cytokines in ischemia-reperfusion-induced injury in the heart, Exp Clin Cardiol. 10 (2005) 213–222.

[56] L. Cabal-Hierro, P.S. Lazo, Signal transduction by tumor necrosis factor receptors, Cell. Signal. 24 (2012) 1297–1305. doi:10.1016/j.cellsig.2012.02.006.

[57] P.C. Rath, B.B. Aggarwal, TNF-induced signaling in apoptosis, J. Clin. Immunol. 19 (1999) 350–364.

[58] D.J. Hausenloy, A. Tsang, M.M. Mocanu, D.M. Yellon, Ischemic preconditioning protects by activating prosurvival kinases at reperfusion, Am J Physiol Heart Circ Physiol. 288 (2005) H971–6. doi:10.1152/ajpheart.00374.2004.

[59] H. Carvalho, P. Evelson, S. Sigaud, B. Gonzalez-Flecha, Mitogen-activated protein kinases modulate H(2)O(2)-induced apoptosis in primary rat alveolar epithelial cells, J. Cell. Biochem. 92 (2004) 502–513. doi:10.1002/jcb.20070.

[60] X. Wang, K.D. McCullough, T.F. Franke, N.J. Holbrook, Epidermal growth factor receptor-dependent Akt activation by oxidative stress enhances cell survival, J Biol Chem. 275 (2000) 14624–14631. doi:10.1074/jbc.275.19.14624.

[61] D. Martin, M. Salinas, N. Fujita, T. Tsuruo, A. Cuadrado, Ceramide and reactive oxygen

species generated by H2O2 induce caspase-3-independent degradation of Akt/protein kinase B, J Biol Chem. 277 (2002) 42943–42952. doi:10.1074/jbc.M201070200.

[62] L. Gallelli, D. Falcone, M. Scaramuzzino, G. Pelaia, B. D'Agostino, M. Mesuraca, et al., Effects of simvastatin on cell viability and proinflammatory pathways in lung adenocarcinoma cells exposed to hydrogen peroxide, BMC Pharmacol Toxicol. 15 (2014) 67. doi:10.1186/2050-6511-15-67.

[63] H. Song, W. Kim, J.-H. Choi, S.-H. Kim, D. Lee, C.-H. Park, et al., Stress-induced nuclear translocation of CDK5 suppresses neuronal death by downregulating ERK activation via VRK3 phosphorylation, Scientific Reports. 6 (2016) 28634. doi:10.1038/srep28634.

[64] Y.J. Kim, J.Y. Kim, S.-W. Kang, G.S. Chun, J.Y. Ban, Protective effect of geranylgeranylacetone against hydrogen peroxide-induced oxidative stress in human neuroblastoma cells, Life Sciences. 131 (2015) 51–56. doi:10.1016/j.lfs.2015.04.009.

[65] J. Zhou, T. Du, B. Li, Y. Rong, A. Verkhratsky, L. Peng, Crosstalk Between MAPK/ERK and PI3K/AKT Signal Pathways During Brain Ischemia/Reperfusion, ASN Neuro. 7 (2015) 175909141560246. doi:10.1177/1759091415602463.

[66] R. Seger, E.G. Krebs, The MAPK signaling cascade, Faseb J. 9 (1995) 726–735.

[67] C. Li, W.-J. Zhang, B. Frei, Quercetin inhibits LPS-induced adhesion molecule expression and oxidant production in human aortic endothelial cells by p38-mediated Nrf2 activation and antioxidant enzyme induction, Redox Biology. 9 (2016) 104–113. doi:10.1016/j.redox.2016.06.006.

[68] P. Sen, P.K. Chakraborty, S. Raha, p38 mitogen-activated protein kinase (p38MAPK) upregulates catalase levels in response to low dose H2O2 treatment through enhancement of mRNA stability, FEBS Letters. 579 (2005) 4402–4406. doi:10.1016/j.febslet.2005.06.081.

[69] D.K.C. Cooper, B. Ekser, C. Burlak, M. Ezzelarab, H. Hara, L. Paris, et al., Clinical lung xenotransplantation--what donor genetic modifications may be necessary?

1 Xenotransplantation. 19 (2012) 144–158. doi:10.1111/j.1399-3089.2012.00708.x.

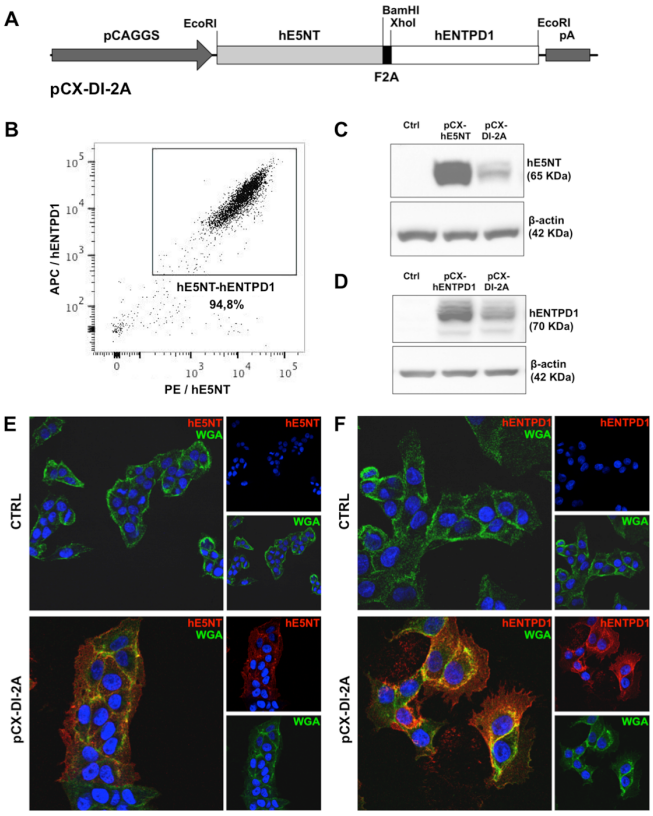
A
pCAGGS
EcoRI
hE5NT
BamHI
XhoI
hENTPD1
EcoRI
pA
F2A
pCX-DI-2A
B
APC / hENTPD1
PE / hE5NT
hE5NT-hENTPD1
94,8%
C
Ctrl
pCX-hE5NT
pCX-DI-2A
hE5NT (65 KDa)
β-actin (42 KDa)
D
Ctrl
pCX-hENTPD1
pCX-DI-2A
hENTPD1 (70 KDa)
β-actin (42 KDa)
E
CTRL
pCX-DI-2A
hE5NT
WGA
F
CTRL
pCX-DI-2A
hENTPD1
WGA

Figure 1.

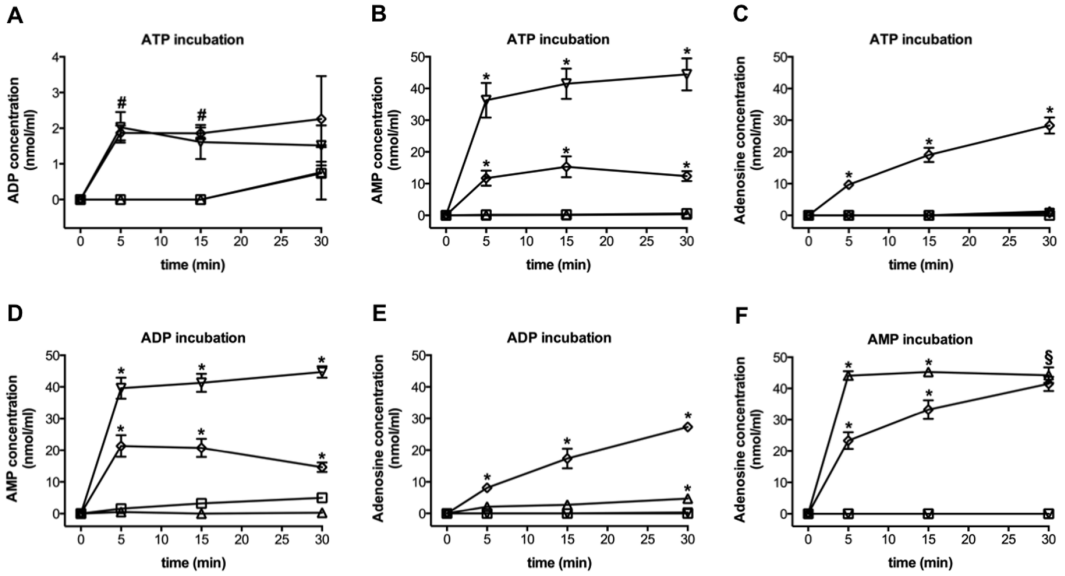
A
ATP incubation
ADP concentration (nmol/ml)
time (min)
B
ATP incubation
AMP concentration (nmol/ml)
time (min)
C
ATP incubation
Adenosine concentration (nmol/ml)
time (min)
D
ADP incubation
AMP concentration (nmol/ml)
time (min)
E
ADP incubation
Adenosine concentration (nmol/ml)
time (min)
F
AMP incubation
Adenosine concentration (nmol/ml)
time (min)

Figure 2.

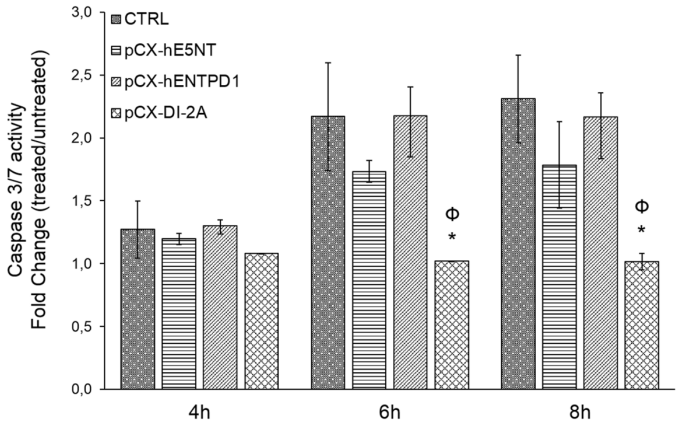
CTRL
pCX-hE5NT
pCX-hENTPD1
pCX-DI-2A
Caspase 3/7 activity
Fold Change (treated/untreated)
3,0
2,5
2,0
1,5
1,0
0,5
0,0
4h
6h
8h
Φ
*
Φ
*

Figure 3.

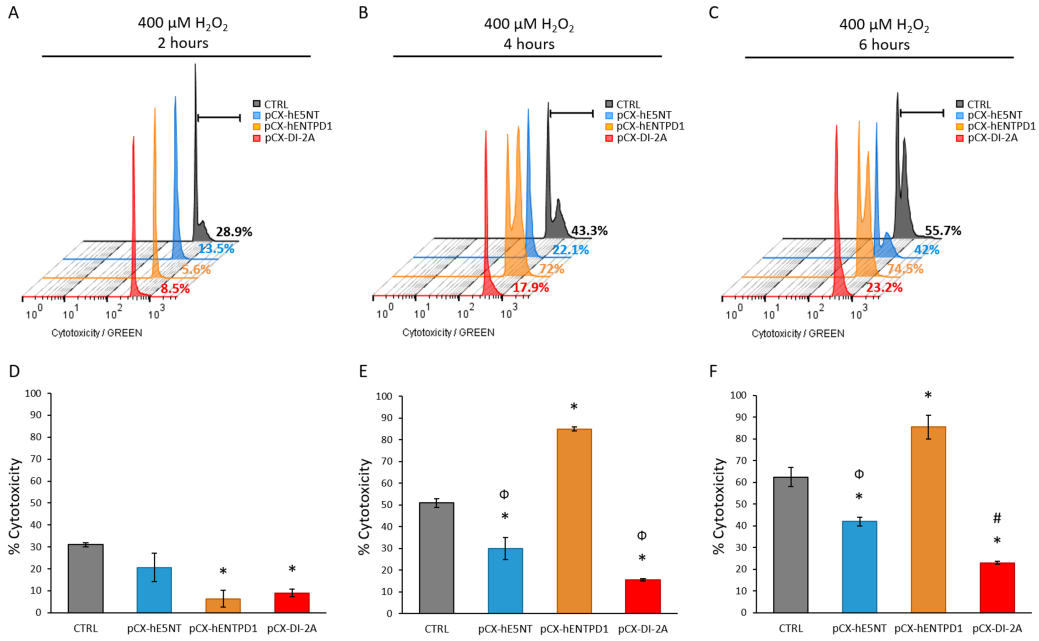
A
400 µM H2O2
2 hours
CTRL
pCX-hE5NT
pCX-hENTPD1
pCX-DI-2A
28.9%
13.5%
5.6%
8.5%
Cytotoxicity / GREEN
B
400 µM H2O2
4 hours
43.3%
22.1%
7.2%
17.9%
C
400 µM H2O2
6 hours
55.7%
42%
14.5%
23.2%
D
% Cytotoxicity
E
F
CTRL
pCX-hE5NT
pCX-hENTPD1
pCX-DI-2A

Figure 4.

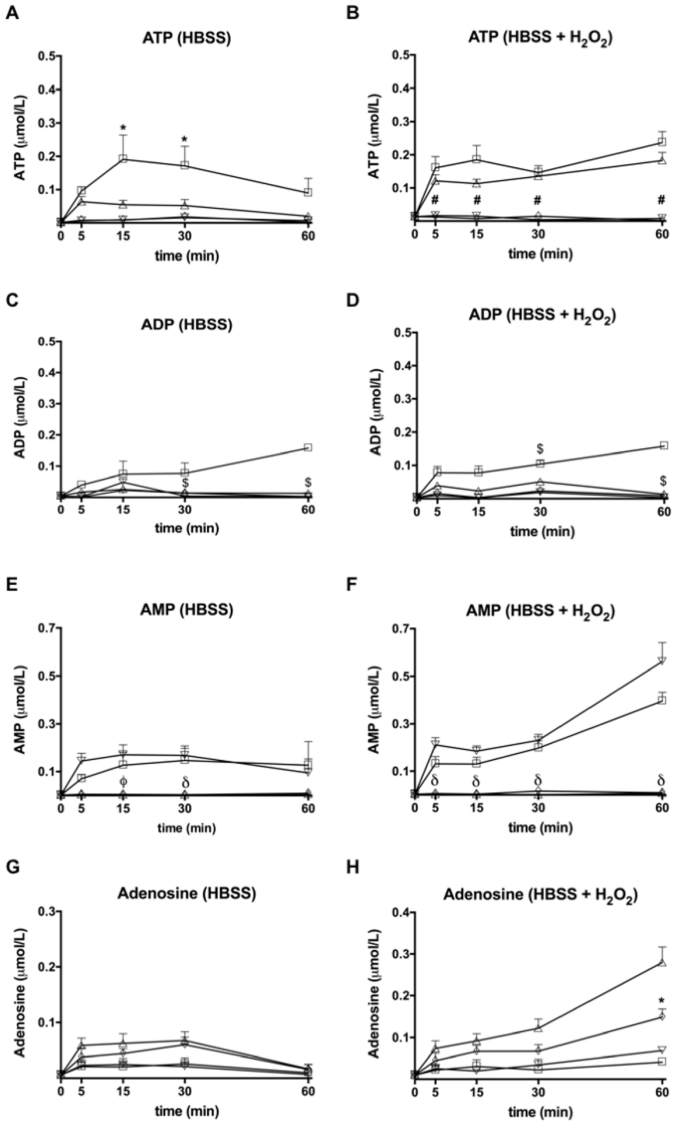
A
ATP (HBSS)
ATP (µmol/L)
time (min)
B
ATP (HBSS + H_2O_2)
ATP (µmol/L)
time (min)
C
ADP (HBSS)
ADP (µmol/L)
time (min)
D
ADP (HBSS + H_2O_2)
ADP (µmol/L)
time (min)
E
AMP (HBSS)
AMP (µmol/L)
time (min)
F
AMP (HBSS + H_2O_2)
AMP (µmol/L)
time (min)
G
Adenosine (HBSS)
Adenosine (µmol/L)
time (min)
H
Adenosine (HBSS + H_2O_2)
Adenosine (µmol/L)
time (min)

Figure 5.

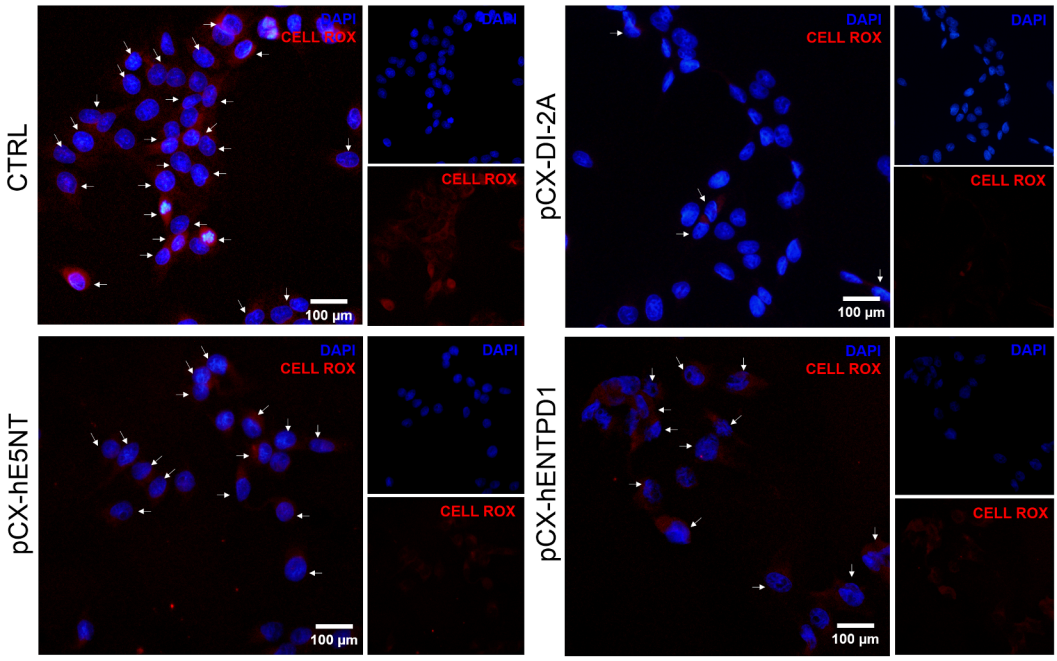

Figure 6.

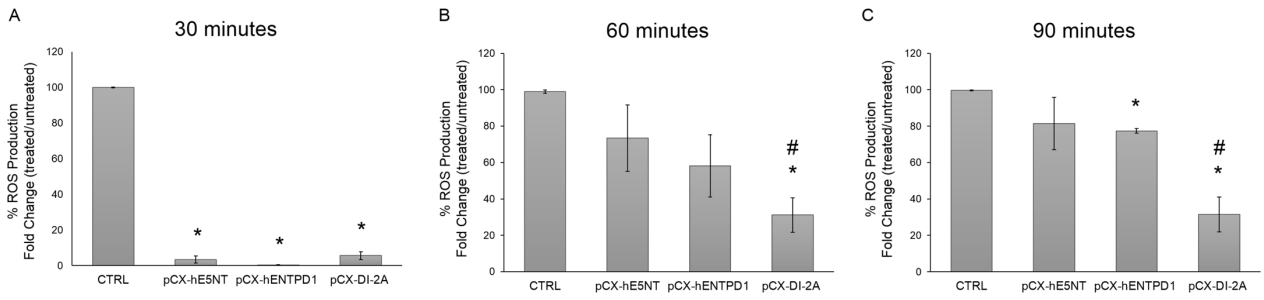
A
30 minutes
% ROS Production
Fold Change (treated/untreated)
120
100
80
60
40
20
0
CTRL
pCX-hE5NT
pCX-hENTPD1
pCX-DI-2A
*
*
*
B
60 minutes
% ROS Production
Fold Change (treated/untreated)
CTRL
pCX-hE5NT
pCX-hENTPD1
pCX-DI-2A
#
*
C
90 minutes
% ROS Production
Fold Change (treated/untreated)
CTRL
pCX-hE5NT
pCX-hENTPD1
pCX-DI-2A
*
#
*

Figure 7.

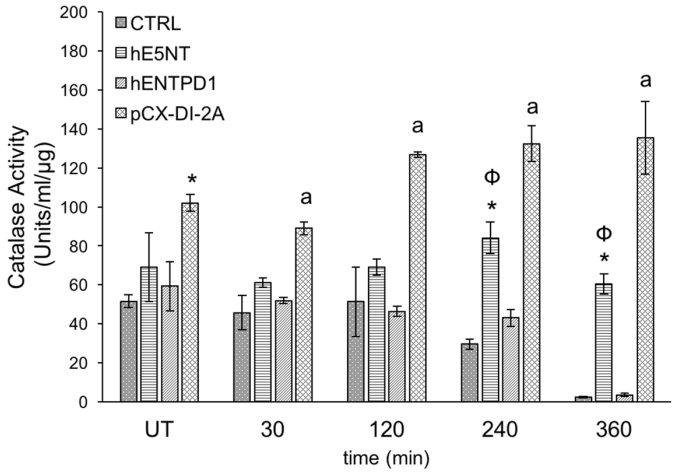
CTRL
hE5NT
hENTPD1
pCX-DI-2A
Catalase Activity (Units/ml/µg)
200
180
160
140
120
100
80
60
40
20
0
UT
30
120
240
360
time (min)
*
a
a
Φ
*
a
Φ
*
a

Figure 8.

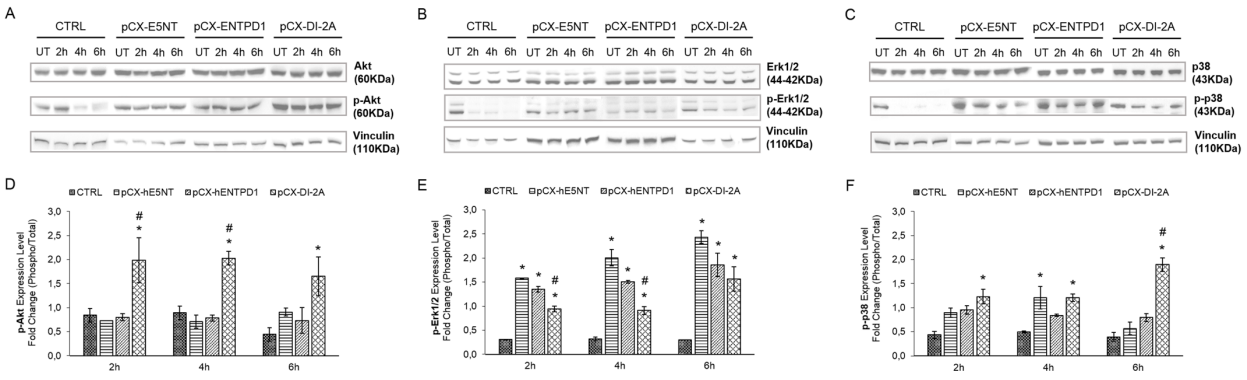
A
CTRL
pCX-E5NT
pCX-ENTPD1
pCX-DI-2A
UT 2h 4h 6h
Akt (60KDa)
p-Akt (60KDa)
Vinculin (110KDa)
B
Erk1/2 (44-42KDa)
p-Erk1/2 (44-42KDa)
Vinculin (110KDa)
C
p38 (43KDa)
p-p38 (43KDa)
Vinculin (110KDa)
D
CTRL
pCX-hE5NT
pCX-hENTPD1
pCX-DI-2A
p-Akt Expression Level Fold Change (Phospho/Total)
2h
4h
6h
E
p-Erk1/2 Expression Level Fold Change (Phospho/Total)
F
p-p38 Expression Level Fold Change (Phospho/Total)

Figure 9.

FRBM – Chisci E., De Giorgi M., *et al*. – Supplementary Material and Methods

Dicistronic plasmid construction

An Eppendorf Mastercycler EP silver block thermocycler was used for synthesizing DNA by PCR reaction. Two rounds of recombinant PCR were performed to amplify hE5NT (NCBI: NM_002526.3) coding sequence (CDS). Firstly, hE5NT CDS was PCR-amplified from pCX-hE5NT (previously produced in our lab) without the stop codon by using EcoRI Kozak hE5NT forward and BamHI hE5NT reverse primers and the corresponding amplicon was cloned into pGEM T-easy vector (Promega). This intermediate vector was used as template for the second PCR, which was performed using AflII hE5NT forward and BamHI hE5NT reverse primers. The corresponding product was cloned into pGEM T-easy vector. Then, the entire CDS was excised by AflII/BamHI double digestion and cloned into AflII/BamHI-digested pcDNA3.1-F2A upstream of F2A sequence, obtaining pcDNA3.1-hE5NT-F2A. hENTPD1 (NCBI: NM_001776.5) CDS was PCR-amplified and then ligated in XhoI/XbaI-digested pcDNA3.1-hE5NT-F2A as previously described[1], obtaining pcDNA3.1-hE5NT-F2A-hENTPD1. The dicistronic cassette hE5NT-F2A-hENTPD1 was excised by EcoRI digestion and ligated in EcoRI-linearized pCX-C1 plasmid [2] acceptor obtaining pCX-hE5NT-F2A-hENTPD1, which was named pCX-DI-2A.

References

[1] M. De Giorgi, A. Cinti, I. Pelikant-Malecka, E. Chisci, M. Lavitrano, R. Giovannoni, et al., Co-expression of functional human Heme Oxygenase 1, Ecto-5′-Nucleotidase and ecto-nucleoside triphosphate diphosphohydrolase-1 by “self-cleaving” 2A peptide system, Plasmid. 79 (2015) 22–29. doi:10.1016/j.plasmid.2015.03.004.

[2] M. Okabe, M. Ikawa, K. Kominami, T. Nakanishi, Y. Nishimune, “Green mice” as a source of ubiquitous green cells, FEBS Letters. 407 (1997) 313–319. doi:10.1016/S0014-5793(97)00313-X.

Supplementary Table 1: List of F2A sequence and primers used for recombinant PCR

Name	Sequence (5'-3')	Tm
F2A-*sense*	GATCCGTGAAACAGACTTTGAATTTTGACCTTCTC AAGTTGGCGGGAGACGTGGAGTCCAACCCAGGG CCCGGCAGCGGCC	
F2A-*antisense*	TCGAGGCCGCTGCCGGGCCCTGGGTTGGACTCC ACGTCTCCCGCCAACTTGAGAAGGTCAAAATTCA AAGTCTGTTTCACG	
EcoRI Kozak hE5NT fw	GAATTCAGGATGTGTCCCCGAGCCGC	60°C
BamHI hE5NT rev	GGATCCTTGGTATAAAACAAAGATC	
AflII hE5NT fw	CTTAAGGAATTCAGGATGTGTCCCCG	60°C
BamHI hE5NT rev	GGATCCTTGGTATAAAACAAAGATC	
XhoI hENTPD1 fw	CTCGAGATGGAAGATACAAAGGAGTCTAACG	60°C
EcoRI hENTPD1 rev	GAATTCCTATACCATATCTTTCCAGAAATATGAAG	
hENTPD1 fw	CTCGAGATGGAAGATACAAAGG	59°C
XbaI hENTPD1 rev	TCTAGAGAATTCCTATACCATATCTTTCCAG	

Supplementary Figure 1. Expression analysis of single gene-transfected cells. (A) FACS analysis of hE5NT (PE) in pCX-hE5NT-transfected cells (black histogram); (B) FACS staining of hENTPD1 (APC) in pCX-hENTPD1-transfected cells (black histogram). Mock-transfected cells were used as negative control (grey histograms in A and B).

Supplementary Figure 2. Efficient catabolism of extracellular adenine nucleotides in pCX-DI-2A-transfected cells. pCX-DI-2A- (◊), pCX-hE5NT- (Δ), pCX-hENTPD1- (∇) and mock- (•) transfected cells were incubated with 50 μM ATP, or ADP, or AMP. The enzymatic degradation of ATP (A), ADP (B) and AMP (C) was measured over different time points by reverse phase HPLC. Error bars represent SEM (n=3). * $p<0.05$ versus all groups; # $p<0.05$ pCX-DI-2A-transfected cells versus all groups except pCX-hENTPD1-transfected cells; § $p<0.05$ pCX-DI-2A-transfected cells versus all groups except pCX-hE5NT-transfected cells.

Supplementary Figure 3. Protection against TNF-α-induced apoptosis in pCX-DI-2A-transfected cells. pCX-DI-2A-, pCX-hE5NT-, pCX-hENTPD1- and mock-transfected (CTRL) cells were treated with 10 ng/ml human TNF-α for 8, 16 and 24 hours and apoptosis was measured by caspase 3/7 assay. Caspase activation in each treated cell line was expressed as a fold change value of the corresponding untreated cells. Error bars represent SEM (n≥3). * $p<0.05$ versus CTRL cells; Φ $p<0.05$ versus pCX-hE5NT-transfected cells.

Supplementary Figure 4. ROS production following 100 μM H_2O_2 exposure. pCX-DI-2A-, pCX-hE5NT-, pCX-hENTPD1- and mock-transfected (CTRL) cells were treated with 100 μM H_2O_2 for 30 (A), 60 (B) and 90 (C) minutes and ROS levels were detected by immunofluorescence staining

with CellROX® Orange Reagent. White arrows indicate cells positive to the staining (red). The bar represents 100 μm. DAPI (blue) was used for nuclear staining. Representative images are shown.

Supplementary Figure 5. ROS production following 400 μM H_2O_2 exposure. pCX-DI-2A-, pCX-hE5NT-, pCX-hENTPD1- and mock-transfected (CTRL) cells were treated with 400 μM H_2O_2 for 30 (A) and 60 (B) minutes and ROS levels were detected by immunofluorescence staining with CellROX® Orange Reagent. White arrows indicate cells positive to the staining (red). The bar represents 100 μm. DAPI (blue) was used for nuclear staining. Representative images are shown.

Supplementary Figure 6. Evaluation of GSH/GSSG ratio in PIEC cells treated with H_2O_2. pCX-DI-2A-, pCX-hE5NT-, pCX-hENTPD1- and mock-transfected (CTRL) cells were treated with 400 μM H_2O_2 for 30, 60 and 90 minutes and GSH/GSSG ratio was determined as described in Materials and Methods. Data are presented as mean ± SEM (n=3). * $p<0.05$ pCX-hENTPD1-transfected cells vs. all the other untreated cell lines. UT, untreated cells.

Supplementary Figure 7. Enzymatic activity of GPx in PIEC cells treated with H_2O_2. pCX-DI-2A-, pCX-hE5NT-, pCX-hENTPD1- and mock-transfected (CTRL) cells were treated with 400 μM H_2O_2 for 30, 120, 240 and 360 minutes and the GPx enzymatic activity was measured as described in Materials and Methods. The activity is expressed as units of enzyme per ml of reaction. Data are presented as mean ± SEM (n≥3). UT, untreated cells.

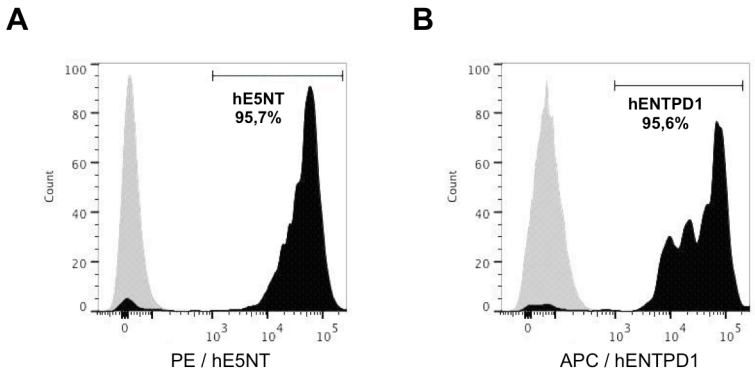

Supplementary Figure 1.

1

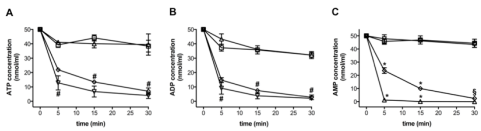

Supplementary Figure 2.

1

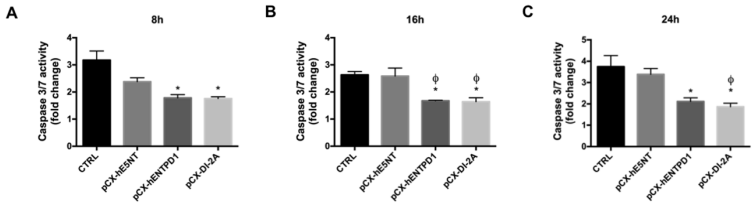

Supplementary Figure 3.

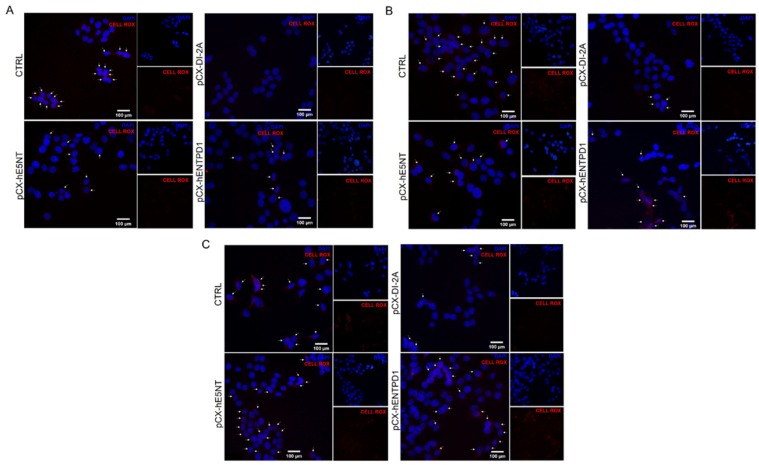

Supplementary Figure 4.

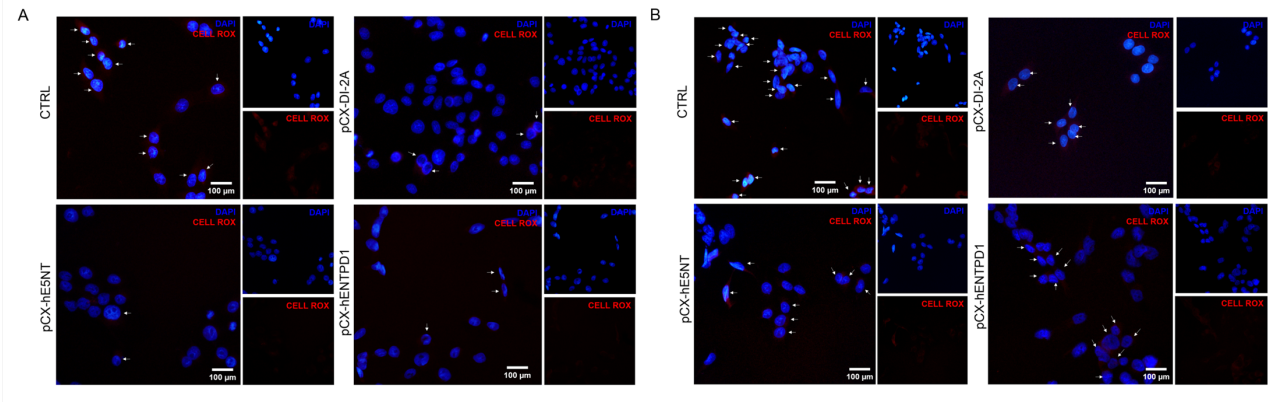

Supplementary Figure 5.

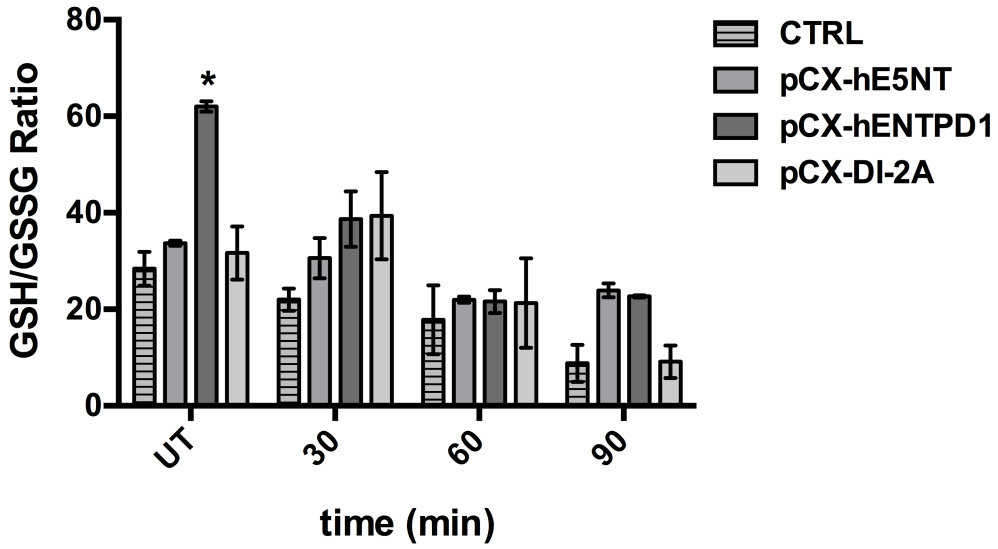

Supplementary Figure 6.

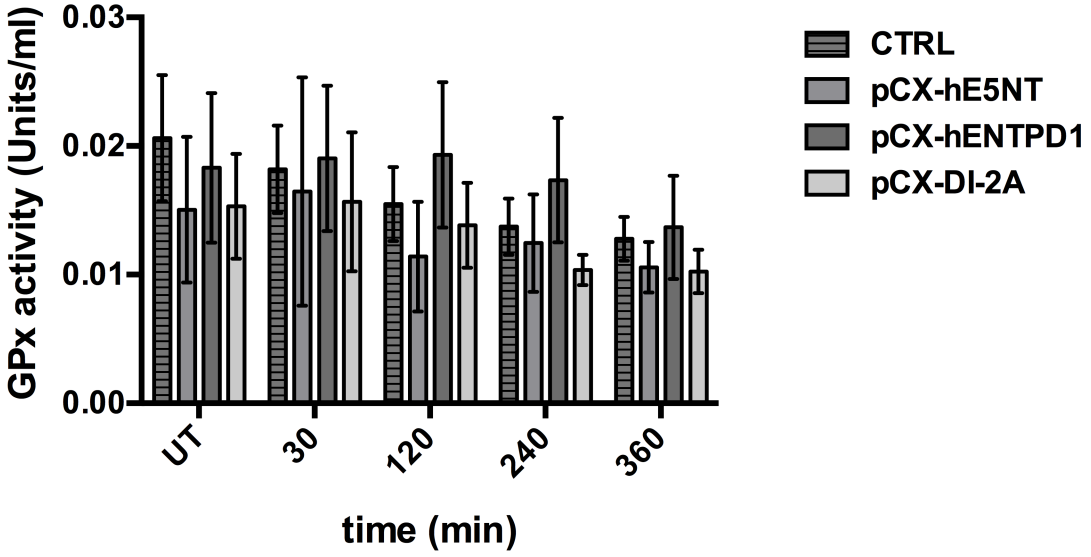

Supplementary Figure 7.